# DEVELOPMENT OF GRAZING INCIDENCE X-RAY DIFFRACTION TECHNIQUE USING SYNCHROTRON LIGHT

**Miskawan Sripukdee**



**A Thesis Submitted in Partial Fulfillment of the Requirements for the Degree of Master of Science in Physics**

**Suranaree University of Technology**

**Academic Year 2018**

# การพัฒนาเทคนิคการเลี้ยวเบนของรังสีเอกซ์ด้วยมุมตกกระทบแบบแฉลบที่ใช้แสงซินโครตรอน

นางสาวมิสกวัน ศรีภักดี



วิทยานิพนธ์นี้เป็นส่วนหนึ่งของการศึกษาตามหลักสูตรปริญญาวิทยาศาสตรมหาบัณฑิต
สาขาวิชาฟิสิกส์
มหาวิทยาลัยเทคโนโลยีสุรนารี
ปีการศึกษา 2561

# DEVELOPMENT OF GRAZING INCIDENCE X-RAY DIFFRACTION TECHNIQUE USING SYNCHROTRON LIGHT

Suranaree University of Technology has approved this thesis submitted in partial fulfillment of the requirements for a Master's Degree

Thesis Examining Committee

(Assoc. Prof. Dr. Puangratana Pairor)
Chairperson

(Assoc. Prof. Dr. Prayoon Songsiriritthigul)
Member (Thesis Advisor)

(Dr. Mati Horprathum)
Member

(Dr. Chomphunuch Songsiriritthigul)
Member

(Prof. Dr. Santi Maensiri)
Vice Rector Academic Affairs and Internationalization

(Assoc. Prof. Dr. Worawat Meevasana)
Dean of Institute of Science

มิสกวัน ศรีภักดี : การพัฒนาเทคนิคการเลี้ยวเบนของรังสีเอกซ์ด้วยมุมตกกระทบแบบแฉลบที่ใช้แสงซินโครตรอน (DEVELOPMENT OF GRAZING INCIDENCE X-RAY DIFFRACTION TECHNIQUE USING SYNCHROTRON LIGHT) อาจารย์ที่ปรึกษา : รองศาสตราจารย์ ดร.ประยูร ส่งสิริฤทธิกุล, 68 หน้า.

วิทยานิพนธ์นี้มุ่งเน้นการพัฒนาเทคนิคการวัดการเลี้ยวเบนของรังสีเอ็กซ์ด้วยมุมตกกระทบแบบแฉลบ (GIXRD)โดยใช้แสงซินโครตรอน เทคนิคดังกล่าวถูกพัฒนาขึ้นที่สถานีทดลองของระบบลำเลียงแสงซินโครตรอน BL7.2W ของสถาบันวิจัยแสงซินโครตรอน โดยแสงที่ได้ในระบบลำเลียงแสงนี้อยู่ในย่านรังสีเอ็กซ์พลังงานสูง ที่ผลิตจากแม่เหล็กเหนี่ยวนำแบบยิ่งยวด (6.5 T Wavelength Sifter) โมโนโครเมเตอร์ชนิดผลึกคู่ถูกใช้เพื่อคัดเลือกพลังงานของรังสีเอ็กซ์โดยครอบคลุมในย่านพลังงานตั้งแต่ 7 ถึง 18 กิโลอิเล็กตรอนโวลต์ อีกทั้งขนาดของลำแสงของรังสีเอ็กซ์สามารถปรับลงในขนาด 20 ไมโครเมตร ทำให้สามารถทำการวัดด้วยมุมตกกระทบแบบแฉลบและนำไปใช้ในการศึกษาระบบผลึกของฟิล์มบางยิ่งยวดได้ รูปแบบการเลี้ยวเบนถูกบันทึกด้วยหัววัดแบบ 2 มิติซึ่งช่วยให้สามารถบันทึกจุดหรือริ้วการเลี้ยวเบนของฟิล์มบางได้มากขึ้น ทั้งนี้ได้ดำเนินการตั้งแต่พัฒนาสถานีทดลองตลอดจนทดสอบการใช้งานของเทคนิคที่ถูกพัฒนาขึ้นด้วยวัสดุสองชนิดคือฟิล์มบางซิงค์ออกไซด์เจือด้วยอะลูมิเนียมและแมงกานีสบิสมัทชนิดผง โดยเทคนิคที่ถูกพัฒนาขึ้นนี้ ได้แสดงให้เห็นถึงประโยชน์ของการวัดการเลี้ยวเบนของรังสีเอ็กซ์ด้วยมุมตกกระทบแบบแฉลบโดยใช้แสงซินโครตรอนนั้นเหนือกว่าการวัดการเลี้ยวเบนของรังสีเอ็กซ์แบบทั่วไป ได้แก่ แสงซินโครตรอนในย่านรังสีเอ็กซ์นั้นมีความเข้มมากกว่ารังสีเอกซ์จากห้องปฏิบัติการทั่วไป ทำให้เวลาที่ใช้ในการวัดสั้นลงเมื่อใช้แสงซินโครตรอน อีกทั้งความสามารถในการปรับค่าพลังงานของแสงซินโครตรอนที่เหมาะสมสำหรับวัสดุแต่ละชนิด และยิ่งไปกว่านั้น หัววัดแบบ 2 มิติที่สถานีทดลองช่วยให้สามารถตรวจวัดการเลี้ยวเบนรังสีเอ็กซ์ของวัสดุได้อย่างหลากหลายประเภท นอกจากนี้ได้มีการพัฒนาเซลล์สำหรับการใส่สารตัวอย่างที่ช่วยให้การวัดสามารถดำเนินไปด้วยการควบคุมเงื่อนไขของฟิล์มบางโดยการให้ความร้อนและป้อนก๊าซที่ต้องการ

สาขาวิชาฟิสิกส์ ลายมือชื่อนักศึกษา มิสกวัน ศรีภักดี

ปีการศึกษา 2561 ลายมือชื่ออาจารย์ที่ปรึกษา

MISKAWAN SRIPUKDEE : DEVELOPMENT OF GRAZING INCIDENCE X-RAY DIFFRACTION TECHNIQUE USING SYNCHROTRON LIGHT. THESIS ADVISOR : ASSOC. PROF. PRAYOON SONGSIRIRITTHIGUL, Ph.D. 68 PP .

GIXRD/XRD/ SYNCHROTRON LIGHT

This thesis focuses on the development of a grazing incidence X-ray diffraction (GIXRD) technique using synchrotron light. The measurement system was developed at the BL7.2W beamline of the Synchrotron Light Research Institute (SLRI). The beamline utilizes X-rays produced from a 6.5 T Wavelength Shifter. A double-crystal monochromator is used to choose X-ray photon energy covering from 7 to 18 KeV. The X-ray beam size can be reduced down to 20 microns, allowing XRD measurements to be carried out in grazing geometry, thus crystal structures of ultra-thin film samples can be investigated. The diffraction patterns are recorded with a 2D CCD detector, allowing more diffraction spots of single crystalline films to be recorded. The development of the GIXRD experimental station was completed. The commissioning of the measurement system was successful with two different types of materials, i.e. aluminium-doped zinc oxide films and manganese bismuth powder. The advantages of synchrotron GIXRD at SLRI over conventional XRD systems have successfully been demonstrated i.e. higher intensity of synchrotron X-rays at the BL7.2W allows much shorter time for the measurements and the tunability of synchrotron X-rays provides a possibility to increase the efficiently of the measurements. Importantly, a 2D detector available at the synchrotron beamline allows more types of materials to be investigated.

In addition, an in-situ cell was designed and constructed. The in-situ cell allows GIXRD measurements to be carried out with the samples in controlled conditions with heating and feeding with required gases for real-time measurements.



School of Physics

Academic Year 2018

Student's Signature ฟิสกัน ศรีภักดี

Advisor's Signature Prayoon Songs.

# ACKNOWLEDGEMENTS

This thesis work would not have been completed without the generous support and invaluable advice from my thesis advisor Assoc. Prof. Dr. Prayoon Songsiririthigul, who has provided me the great opportunities to learn about GIXRD technique and synchrotron beamline instrument. I am very grateful to him for his encouragement and assistance during my master studies. I am also very grateful to thank Assoc. Prof. Dr Sirichok Jungthawan, Dr. Mati Horpratum and Dr. Chomphunuch Songsiririthigul for being my thesis committee. Most of my thesis work was performed at the BL7.2W: MX beamline of the Synchrotron Light Research Institute (Public Organization) of Thailand. I am also very grateful to all staff members of the beamline during the instrument set up, especially, Dr. Chomphunuch Songsirilitthigul for her kind help and advice about technical information and operation of beamline instruments. I would like to express my sincere thanks to Mr. Mongkol Phanak for his kind help in the mechanical design of the GIXRD in-situ cell. I wish to acknowledge the Thailand Center of Excellence in Physics (ThEP) for the financial support. Importantly, I am deeply grateful to the faculties of the school of Physics, Suranaree University of Technology for help and support. Finally, I would like to express thanks to my parents, brother, and sister for great support, advice, and encouragement to me throughout my studies.

Miskawan Sripukdee

# CONTENTS

**Page**

# CONTENTS (Continued)

**Page**

# CONTENTS (Continued)

**Page**

# LIST OF TABLES

**Table** **Page**

# LIST OF FIGURES

**Figure** **Page**

# LIST OF FIGURES (Continued)

# LIST OF FIGURES (Continued)

**Figure** **Page**

# LIST OF ABBREVIATIONS

| | | |
|---|---|---|
| AZO | = | Aluminium-doped zine oxide |
| BL | = | Beamline |
| BM | = | Bending magnet |
| CCD | = | Charge-coupled device |
| CM | = | Collimating mirror |
| DCM | = | Double-crystal monochromator |
| DTB | = | Desktop beamline |
| FM | = | Focusing mirror |
| GIXRD | = | Grazing incidence X-ray diffraction |
| LTP | = | Low-temperature phase |
| MnBi | = | Manganese bismuth |
| MPW | = | Multi-Pole Wiggler |
| PLD | = | Pulsed laser deposition |
| SLRI | = | Synchrotron Light Research Institute (Public Organization) |
| SDD | = | Sample to detector distance |
| SPS | = | Siam Photon Source |
| SWLS | = | Superconducting Wavelength Shifter |
| XRD | = | X-ray diffraction |
| ZnO | = | Zinc oxide |

# CHAPTER I

# INTRODUCTION

X-ray Diffraction (XRD) is the most well-known family of techniques to investigate structural properties of materials. When X-rays passed through a crystal, they are scattered off by the atoms in the sample and then produce constructive interference at specific angle. Conventional X-ray diffractometers (powder diffractometers) typically work on Bragg-Brantano geometry (Kriegner *et al.,* 2015), the incidence angle is defined between the incident X-ray beam and the sample surface, the diffraction angle ($2\theta$) is defined between the incident beam and the reflect beam. In case of very thin films, grazing geometry is essentially required to increase the interaction volume of X-rays with the materials in the films. The measurement with this geometry is known as grazing incidence XRD (GIXRD), which was first demonstrated by Marra *et al.* in 1979 for the investigations of crystalline surface and interface with varying the incidence angle of X-rays with the aim to get total X-ray external reflection from the sample. In GIXRD measurements, the effective size of the X-ray beam on the sample surface is increased and the signal from a substrate is decreased (Colombi *et al.,* 2006). GIXRD measurements can in principle be performed by using X-rays from synchrotron light sources and from X-ray generators in general laboratory (Neuschitzer *et al.,* 2012). However, there are several advantages when using synchrotron X-rays. The small beam size of synchrotron X-rays allows GIXRD measurements to be performed in small area on the sample. The intensity of synchrotron X-ray is much

higher than rotating anode X-ray and, thus, the data collection time is much shorten when using synchrotron X-rays. Moreover, synchrotron X-rays have a continuous spectrum covering a wide spectral range, thus, one can choose any X-ray wavelength suitable for the materials being investigated.

Two different materials will be used for commissioning the GIXRD set-up in this work. Those are MnBi/Mn powders and aluminum-doped zinc oxide (AZO) thin films. The MiBi/Mn powders consists of an Mn core with MnBi shell, which will be prepared by sintering of the mixture of Mn and Bi powders. MnBi is an interesting magnetic material for the hard phase of future rare-earth-free permanent magnet. AZO is a promising transparent conducting oxide for different electronic devices. AZO may be prepared by various technique such as by pulsed laser deposition (PLD) (Ning *et al.*, 1997), sputtering deposition (Lee *et al.*, 2012), spray paralysis (Studenikin *et al*, 1998), sol–gel method (Ohyama *et al.*, 1997). Among those techniques, magnetron sputtering is the widely used technique due to its high deposition speed and excellent film quality (Wang *et al.*, 2011). ZnO thin films deposited by magnetron sputtering usually shows preferential orientation of c-axis, i.e. (002) texture (Zhang *et al.*, 2010; Suchea *et al.*, 2007), which can be used to emphasize the usefulness of the GIXRD set-up in this work.

The GIXRD set-up in this work was developed at beamline BL7.2W:MX (Songsiriritthigul *et al.*, 2016) of the Synchrotron Light Research Institute (Public Organization) SLRI. A two-dimensional CCD detector was used, which allows diffraction spots outside the plane of incidence to be recorded. In addition, the salient properties of synchrotron X-rays, data acquisition time is shortened by using the CCD detector.

The main goal of this thesis work is to develop GIXRD technique for investigations of ultra-thin films. The setup was also be used for the investigation of powders with Mn core and MnBi shell. In addition, this thesis work involved in the development of the GIXRD in-situ cell, which is the instrument used for real-time characterization of thin films. Participation in the design, construction and commissioning of the GIXRD experimental station provided an opportunity to be trained and get experience on the development of synchrotron instrumentation, control/data acquisition technology, as well as beamline technology. The scope of this work is, of course, on an X-ray diffraction technique.

# CHAPTER II

# LITERATURE REVIEW

This chapter gives a brief historical background of X-rays, source of X-rays, applications and theory of X-ray diffraction technique. Furthermore, knowing about the geometry of X-ray diffraction is essential for achieving the setting up of GIXRD technique. Description of two different materials (AZO thin film and MnBi powder) that were chosen for the commissioning the GIXRD system are also described in this chapter.

## 2.1 History of X-rays

X-rays and their applications have more than a hundred years of history and being continuously developed to be utilized in a variety of fields. X-rays were discovered by the German physicist Wilhelm Conrad Röntgen in 1895, working with cathode-ray tube in his laboratory. The mysterious light was found to be invisible to human eyes, but capable of penetrating opaque objects and exposing photographic films. He received the Nobel Prize in Physics for his discovery in 1901. X-ray diffraction technique was developed by Max von Laue and W.L. Bragg in 1912 and W.H. Bragg in 1913. At first, X-ray diffraction was used only for determining crystal structures. Later on, this technique was continuously improved and applied not only to

structure determination but to such diverse problems as traces measurement, study of phase transition, analysis of particle size and determination of the orientation of one crystal or the ensemble of orientations in materials science.

## 2.2 X-rays sources

### 2.2.1 Laboratory X-rays sources

X-rays are classified as electromagnetic waves and having a wavelength between 1Å to 0.01Å. X-rays are generated conventionally using an X-ray tube. X-ray tubes consist of a source of electrons, a high accelerating voltage and a metal target, as shown in figure 2.1. When the filament of cathode side was heated up by the current. Electrons are emitted from the cathode and accelerated by the high voltage between the cathode and anode (metal target). When the electron beam hits the target, X-ray are produced. X-rays that were produced are consist of a maximum of different wavelengths and variation of intensity (figure 2.2a). If the electron has enough energy it can knock an orbital electron out of the inner electron shell of metal atom, electron from higher energy levels then fill up the vacancy and X-ray photon are emitted appear as a characteristic X-ray spectrum (figure 2.2b). X-ray energy that emits by this process is specific for each element due to that an element has a unique set of electron binding energies.

### 2.2.2 Synchrotron X-rays sources

Synchrotron light source is another type of an X-ray source. Synchrotron X-rays are produced by accelerating charged particles, mostly electrons due to its light weight, thus making them easier to be accelerated to nearly the speed of light. These relativistic electrons are then deflected by a magnetic field, causing them to lose some

of their energy in the form of electromagnetic wave. The unique properties of synchrotron light are summarized as follows.

**Broad spectrum and tunability**: The spectrum that of synchrotron radiation from bending magnet and wiggler are continuous and covers from microwaves to hard X-rays depending on electron energy and the magnetic field. The tunability provides the flexibility in choosing suitable photon energy for several types of experiments by the use of a monochromator. For synchrotron X-rays, most commonly used monochromator is a double crystal monochromator. Silicon and germanium single crystal are normally employed. The photon energy of X-rays is chosen by rotating the crystal to alter θ (the incident angle of synchrotron white beam and crystal plane) under Bragg' s condition (Catlow *et al.*, 1990). This makes synchrotron light favorable for a wide variety of research fields.

**High collimation and low emittance**: (The divergence of synchrotron X-ray in the order of μrad.) this results in less wastage of radiation in its passage through the optical components towards the sample, and greater eventual resolution in measurement due to its spatial precision.

**High brilliance**: Due to the fact that synchrotron has X-ray beam very low divergence and small beam size this leads to it has a high flux intensity with many orders of magnitudes comparing with conventional X-rays thus allowing data to be collected rapidly.

X-rays are applied and useful in various fields. In medical imaging, by using ionizing radiation of X-rays to generate an image of the body (CT scan). Industrially, X-rays can be used to ensure the quality of fabrications throughout production.

Moreover, X-rays are played an important role in material science to solve and diverse the problems as a trace measurement.

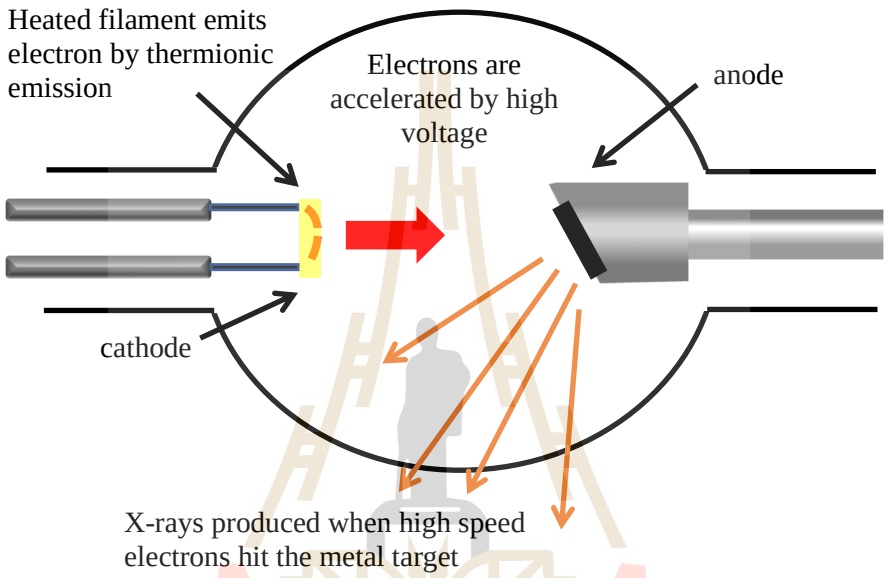


**Figure 2.1** Schematic of X-ray tube (Cullity, 1978).

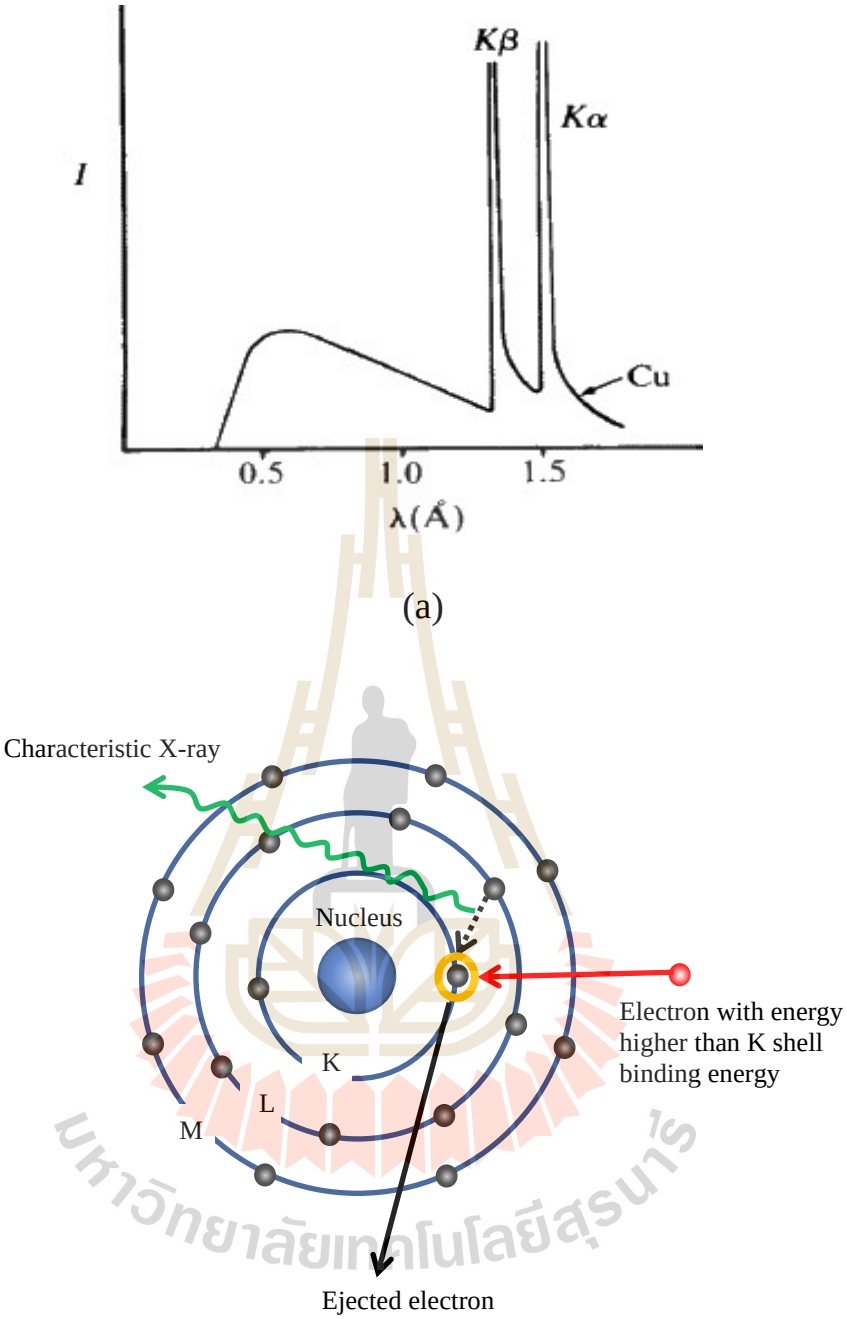


**Figure 2.2** (a) The spectrum consists of continues radiation and characteristic radiation lines Kγ and $K_\beta$ of Cu from (Yoshio *et al.*, 2011) and (b) The mechanism of the characteristic X-ray generations.

## 2.3 X-ray diffraction (XRD)

X-rays are one type of electromagnetic radiation with very short wavelengths. When the X-rays on reaching a material, some of X-rays are absorbed and some scattered. If neither process occurs, the X-rays penetrate through the materials. Scattering can be either elastic and inelastic, elastic scattering occurs when there is no change energy between the incident photon and the emitted photon. Conversely, inelastic scattering involves photon energy loss. X-ray diffraction involves only with elastic scattering. Upon the X-rays plane wave falling on to the atomic of a crystal planes, the reflected X-rays interference pattern then produces. If the waves are in phase, then constructive interference occurs. If the waves are out of phase, then deconstructive interference occurs. For a measurable diffracted beam complete destructive interference does not occur. The regularly-spaced atoms in a crystal lattice causes the X-rays to be diffracted, producing the well-known XRD patterns. Mathematically, XRD signal is best-known to follow Bragg's Law for constructive interference

$$2d\sin\theta = n\lambda \tag{2.1}$$

where $d$ is the separation between the Bragg planes, $\theta$ is the Bragg angle, $n$ is the diffraction order, and $\lambda$ is the X-ray wavelength. The term Bragg planes refer to planes that are included of these constructively diffracting atoms.

### 2.3.1 Conventional of XRD measurement geometry

A typical XRD system consists of a source of radiation, a monochromator to choose the wavelength, slits to adjust the shape of the beam, a sample and a detector. In a more complicated apparatus, a goniometer can also be used for fine adjustment of the sample and the detector positions. When an area detector is used to monitor the diffracted radiation, a beam-stop is usually needed to stop the intense primary beam that has not been diffracted by the sample, otherwise the detector might be damaged. Diffractometers can be operated both in transmission and reflection, but reflection is more common. The sample is loaded in a small disc-like container and its surface carefully flattened. The disc is put on one axis of the diffractometer and tilted by an angle ω while a detector around it on an arm at twice this angle. This configuration is known under the name Bragg–Brentano ω-2θ. Another configuration is the Bragg–Brentano ω-θ configuration, as shown in figure 2.4, in which the sample is stationary while the X-ray tube and the detector are rotated around it. The angle formed between the tube and the detector is 2θ.

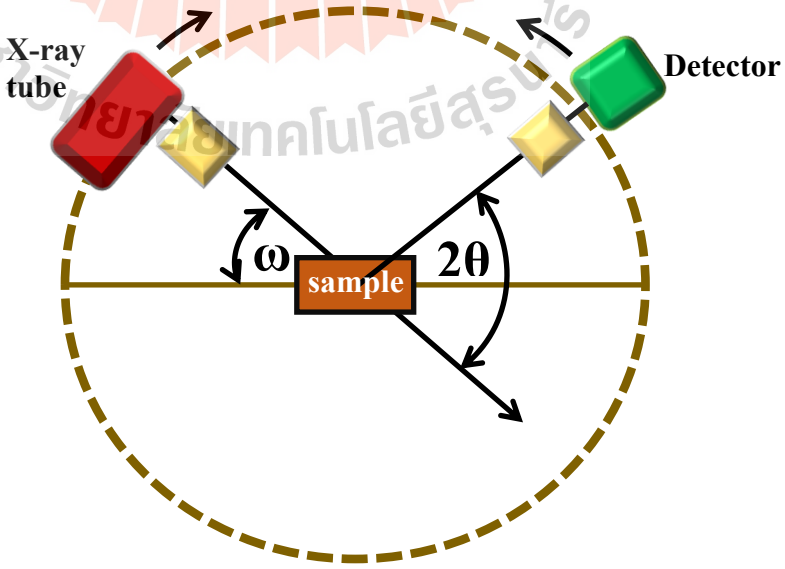


**Figure 2.3** Schematic of Bragg–Brentano θ-θ geometry.

### 2.3.2 GIXRD measurement geometry

Grazing incidence configurations have been developed to overcome limitations of conventional XRD. With a fixed very low incidence angle, X-rays with large grazing angles of incidence penetrates through a few to several hundred micrometers inside the material under investigation, when it comes to thin film analysis the beam penetration depth may be much greater than the sample thickness seen in figure 2.4(a). Hence, conventional XRD is not suitable for detailed study of sub-micrometric layers in thin film specimens. The grazing measurement geometry is particularly useful for increasing signal yield by increasing the irradiated volume, especially in the case of thin film samples. It also has the added benefit of reducing irradiated substrate volume see in figure 2.4(b). Many researches employed GIXRD technique to study structure of thin films. By means of GIXRD experiments, information on sample structure (thickness, phase, etc.) (Golovin *et al.*, 1985; Dosch *et al.*, 1988; Wang *et al.*, 2005) and microstructure (strain field, preferred orientation, etc.) (Williams *et al.*, 1991; Satapathy *et al.*, 2005) at the surface can be simultaneously obtained.

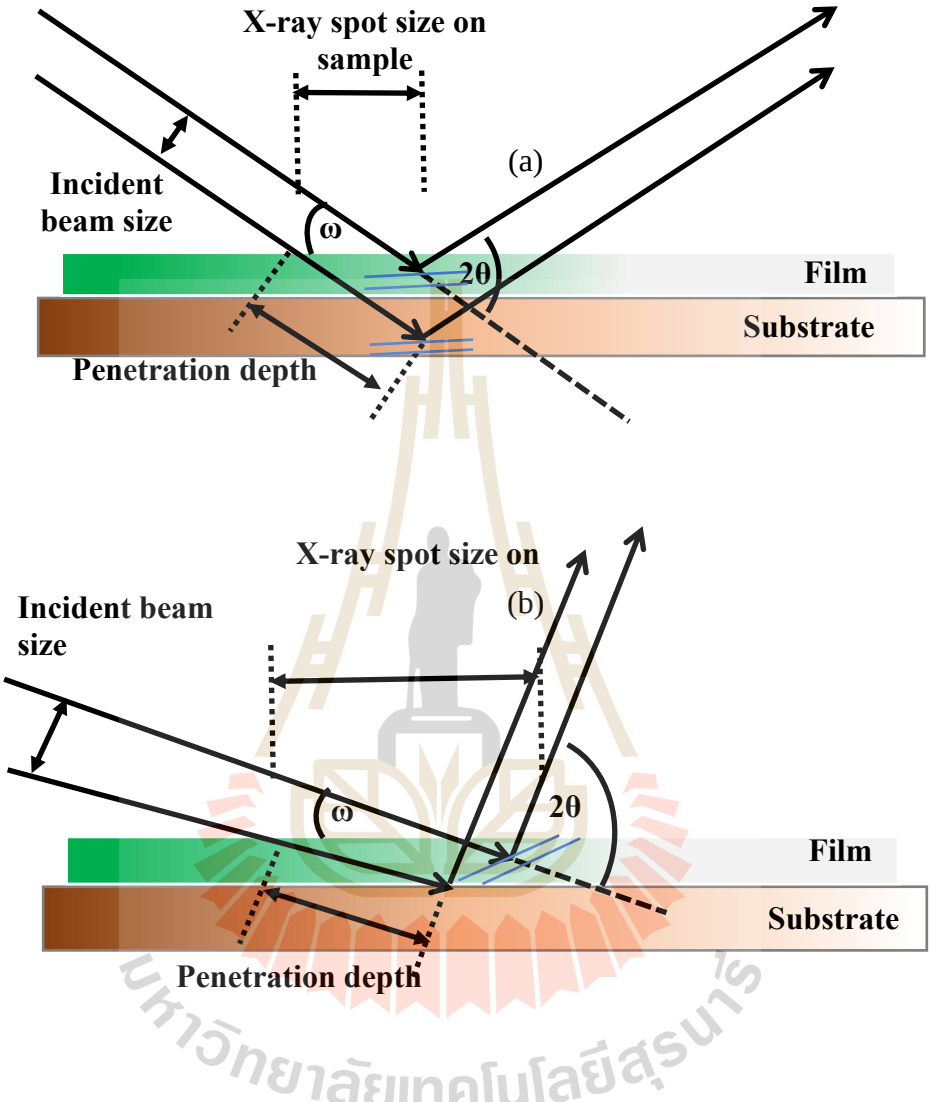


**Figure 2.4** Illustration of GIXRD (a) Illustration of XRD done at a high incident angle on a thin film. (b) The same measurement but done at low incident angle (Widjonarko, 2016).

## 2.4 Crystal structures

Solid materials can be classified into three general categories: single crystal, polycrystalline and amorphous. Figure 2.5 presents simple schematics of these three categories. The largely ordered parts of the materials are called crystallites. In single crystal, the crystal lattice of the entire sample is continuous and no grain boundaries. A polycrystalline material consists of many small single-crystal regions separated by grain boundaries. The grains on either side of the grain boundary are misoriented with respect to each other. For a material that has a largely disordered parts are called amorphous. Naturally, the focus of any investigation on structural properties of a material is measuring the degree of order or disorder in the atomic placements inside the sample. In a crystallite, atoms are spatially placed in a regular interval called the crystal's "lattice parameters". In three-dimensional crystals, these are comprised of a set of three lattice vectors (a, b, c) and 3 angles (α, β, γ) (Clegg *et al.*, 2001). Lattice parameters are the most important physical quantity in XRD as periodicity in atomic placement is the physical property that gives rise to XRD peaks and the set of lattice parameters is unique to every crystal composition.

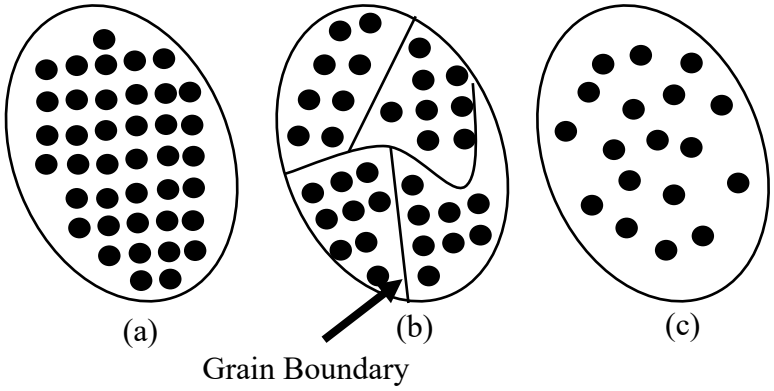


**Figure 2.5** Schematic of (a) Single crystal, (b) polycrystalline and (c) amorphous materials.

## 2.5 Materials for commissioning

MnBi/Mn and AZO were the materials for commissioning the GIXRD set-up. The main work was focused on AZO thin films on Si or glass substrates since thin films are the most suitable material system for GIXRD technique.

### 2.5.1 Aluminium-doped Zinc Oxide (AZO)

Zinc oxide (ZnO) had been actively investigated as an alternative to transparent conducting oxide film due to zinc oxide is a non-toxic, inexpensive and abundant material. ZnO can be modulated by doping with appropriate elements to improve its optical and electrical characteristics. To achieve a low resistivity (high transmittance) in the visible region, the ZnO is usually doped with group III elements such as gallium (Ga), aluminum (Al) and etc. ZnO thin films deposited by magnetron sputtering usually shows preferential orientation of c-axis, i.e. (002) texture (Pan *et al.,* 2012) (Zhang *et al.,* 2010) (Suchea *et al.,* 2017) and some researchers found that in some cases (103) texture could exist (Wang *et al.,* 2012) (Lee *et al.,* 2012). Wang *et al.* employed GIXRD to investigate an appearance of the (103) diffraction in a magnetron

sputtering system of AZO films. Figure 2.6 shows XRD and GIXRD pattern of AZO film, the (103) peak just showed up in GIXRD patterns and when the incidence angle (ω) increased from 2° to 10°, the ratio of I(103)/I(002) became smaller in Figure 2.6(b). They suggested the origin of (103) peak was related with the surface structure because of the GIXRD presents more details of surface information than XRD and smaller incidence angle guarantees more details of surface information than the bigger angle.

### 2.5.2 MnBi/Mn

Recently, rare earth free permanent magnet was developed continuously due to the limited resources of rare earth elements (Mikio *et al.*, 1997). MnBi is the one of magnetic materials for the hard phase of a future rare-earth-free permanent magnet. It was reported that MnBi with low-temperature phase (LTP) have higher values of coercivity (Moon *et al.*, 2014); (Saha *et al.*, 2002); (Ly *et al.*, 2014) which is prepared in various method. It is difficult to obtain the single phase LTP MnBi due to the difference of melting point between Mn(~1246°C) and Bi(~271°C). In the development of new materials, characterization techniques are necessary. XRD is one of the important characterization tools for the development of MnBi magnetic material. In this work, the MiBi/Mn powders consists of an Mn core with MnBi shell, which was prepared by sintering of the mixture of Mn and Bi powders in vacuum.

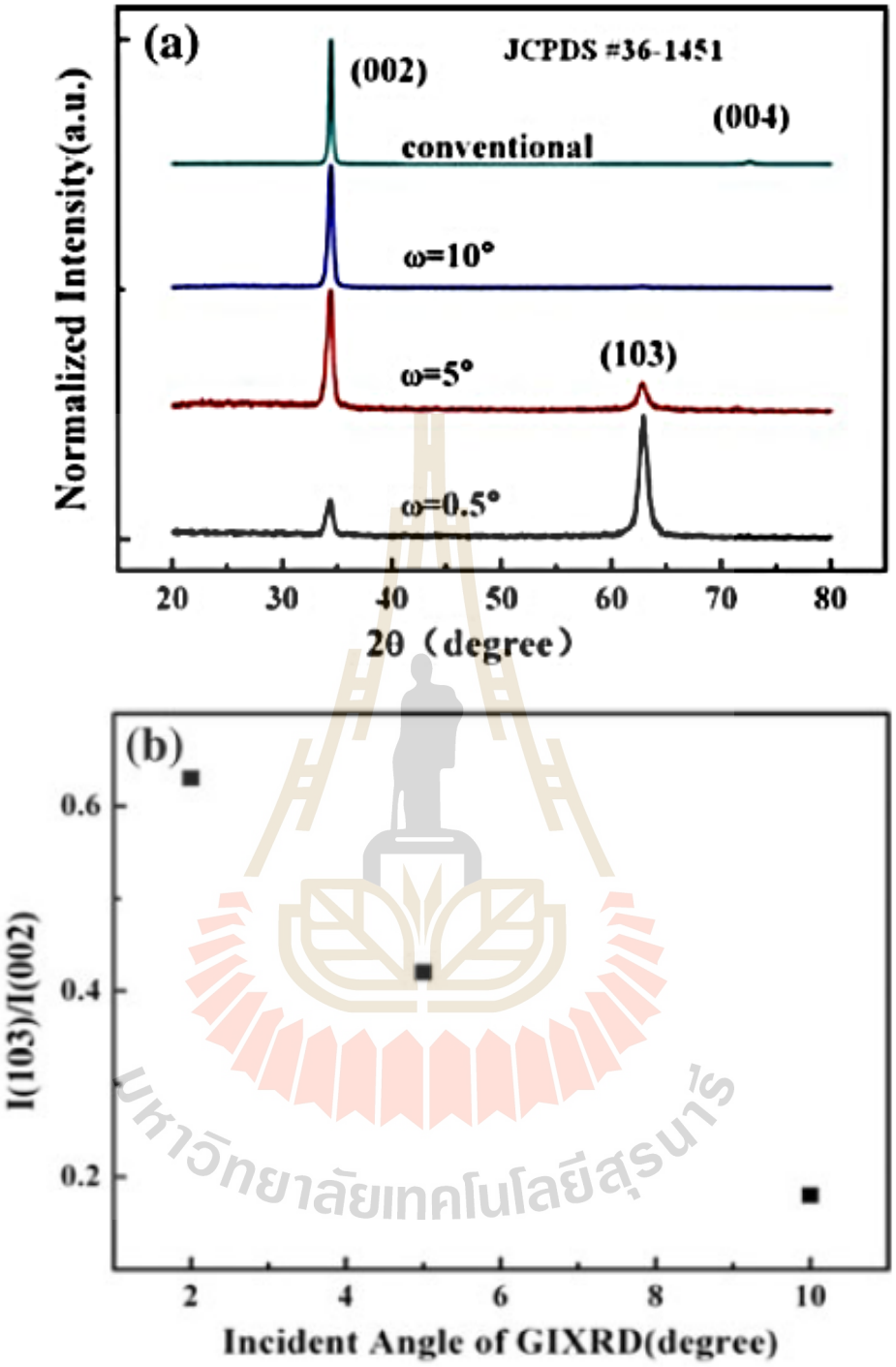


**Figure 2.6** (a) XRD and GIXRD result of AZO film, the incidence angles employed in GIXRD measurements were 0.5°, 5° and 10° and (b) The ratio of I(103)/I(002) of AZO film (Wang *et al.*, 2012).

# CHEPTER III

# DEVELOPMENT OF GIXRD EXPERIMENTAL STATION

In this chapter, detailed descriptions of the original experimental station and beamline instruments are given. The GIXRD technique was developed at the experimental station of BL7.2W: MX beamline. The measurement techniques of this thesis work are described. This includes the limitation and involvement of sample alignment in GIXRD measurement. The commissioning GIXRD set up are also described. The GIXRD in-situ cell is also developed along the course of this thesis work, which is the instrument used for real-time characterization of thin films. The descriptions of a GIXRD in-situ cell are also provided in this chapter.

## 3.1 Synchrotron light beamline: BL7.2W: MX

The beamline BL7.2W:MX utilizes synchrotron light produced from a 6.5 Tesla Superconducting Wavelength Shifter (SWLS) installed in the 1.2-GeV storage ring of the Siam Photon Source of SLRI. The calculated synchrotron spectra generated from SWLS, as well as from other devices, i.e. a linear undulator with a period of 60 mm (U60), multi-pole wiggler (MPW) and bending magnet (BM), are shown in figure 3.1 (Sudmuang *et al.*, 2014). The beamline can be operated with a hard of X-ray energy range with the order of $10^{10}$ photons/s of photon flux, XRD measurements and with the

facility of the instrument at the beamline, the X-ray beam can be aligned and reduced down to 20 microns. Thus, it allows to setup the GIXRD experiment at the end station of beamline. The side-view drawing and optical layout of the BL7.2W: MX beamline is shown in figure 3.2. Major optical elements of the BL7.2W: MX beamline such as a cylindrical collimating mirror (CM), a commercial double-crystal monochromator (DCM) and a toroidal focusing mirror (FM) (Klysubun *et al.*, 2010) are used to produce a focused hard X-ray beam with required characteristics for diffraction experiments of crystalline samples. Figure 3.3 shows the experimental station of the beamline BL7.2W: MX which consists of a cryo-cooler, sample holder and Mar165 CCD detector system (Rayonix LLC, Evanston, Illinois, USA). The sample holder and the detector are mounted on a MarDTB Goniometer system (Marresearch GmbH, Norderstedt, Germany). The distance between the sample and detector can be varied between 45 to 390 mm.

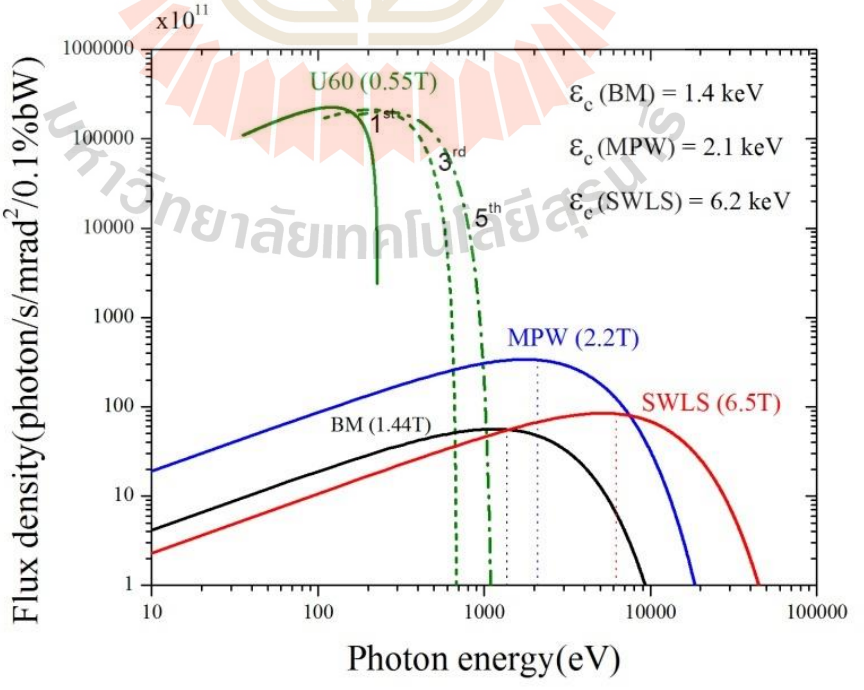


**Figure 3.1** The SPS spectral flux densities. (Sudmuang *et al.*, 2014).

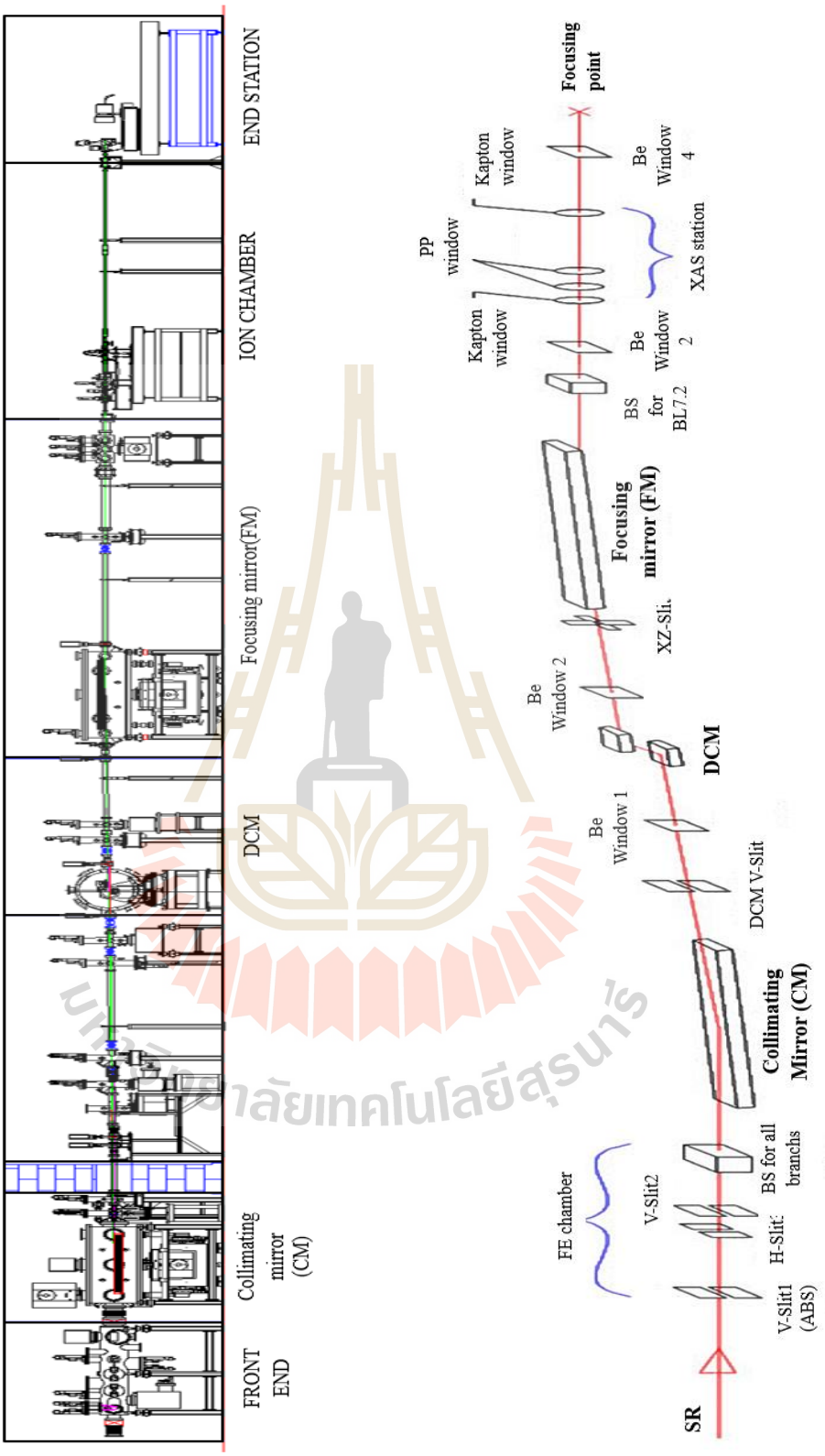


**Figure 3.2** (a) Side-view drawing and (b) Optical layout of the BL7.2W: MX beamline (Songsiriritthigul *et al.*, 2016).

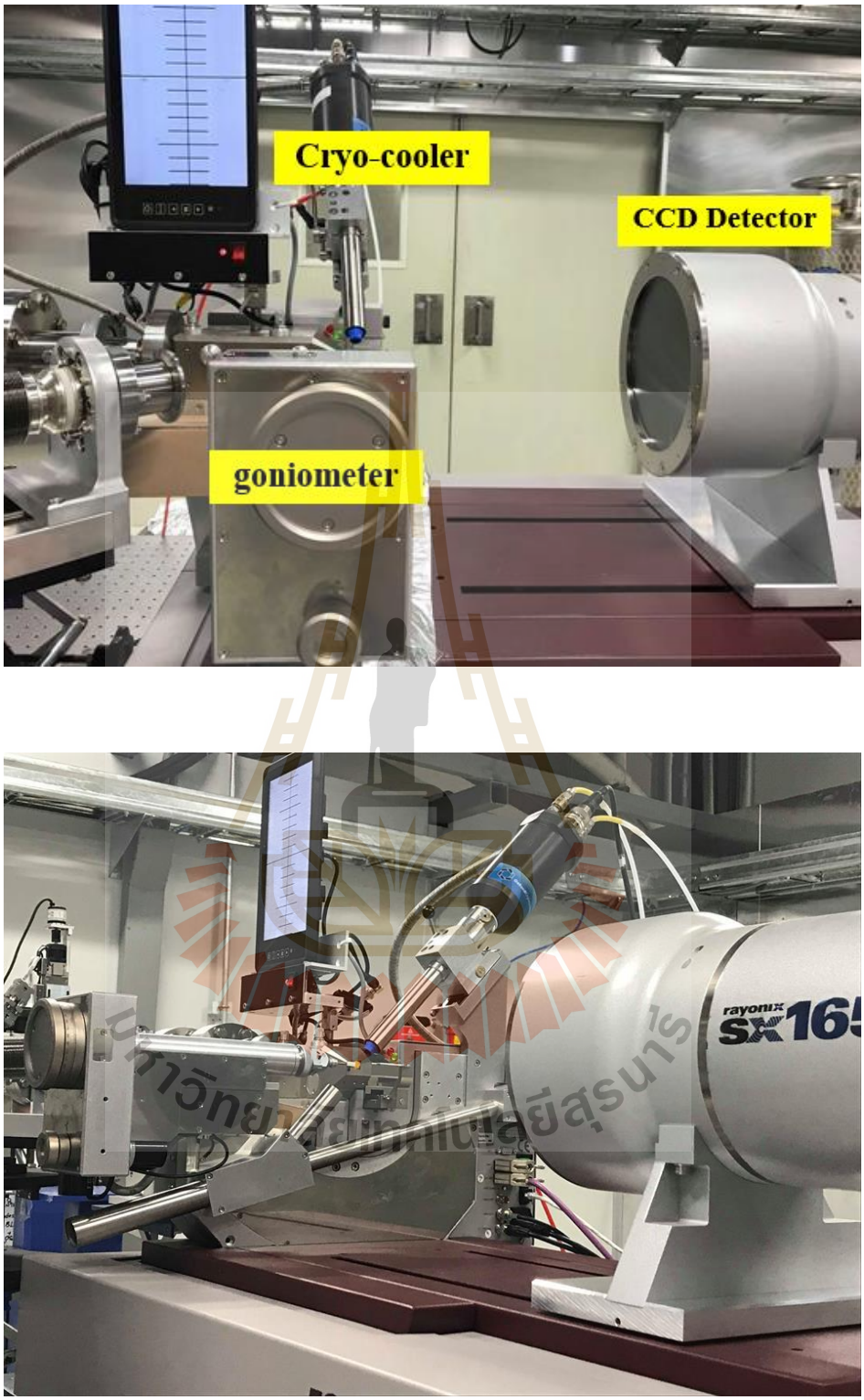


**Figure 3.3** Photo of the experimental station of the BL7.2W:MX beamline.

## 3.2 Existing detector, sample holder & manipulator

Originally, the experimental station of beamline was designed to study structural properties of proteins and macromolecules with synchrotron X-rays. The photon energy range available is between 7 and 18 keV. The detector and sample holder are manipulated with the MarDTB (desktop beamline) goniometer system (Marresearch GmbH, Norderstedt, Germany). Almost all movements are motorized with a highly sophisticated and can be controlled by a host computer. With this system, the detector and sample holder can be aligned with the X-ray beam. In addition, the MarDTB is capable of finding the beam and refining the optimal position thus yielding the best possible primary X-ray beam intensity. The primary X-ray beam passes through the collimator before hitting to a sample that mounts on the PHI-axis. This section consists of two pairs of continuously variable slits followed by an ionization chamber of each see in figure 3.4. The ionization chambers detect the intensity of the primary X-ray beam coming through the slits and the X-ray beam size can be adjusted by driving the 4 motors (vertical, horizontal in front of first ionization chamber and second ionization chamber). In addition, the collimator comprises of a CCD-microscope to viewing direction along the X-ray beam. The beam stop is movable to protect the detector from the primary X-ray beam.

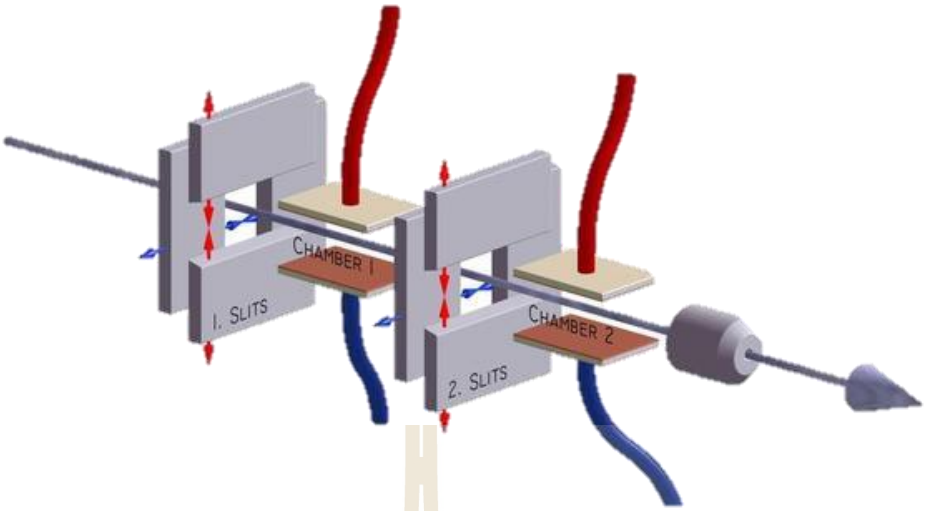


**Figure 3.4** Photo of collimator component on MarDTB system. (Marresearch Gmb, 2001)

## 3.3 A modified sample holder: translation/ration of sample

Figure 3.5 shows the experimental station of BL7.2W: MX beamline which consists of a cryo-cooler, sample holder and Mar165 CCD detector system (Rayonix LLC, Evanston, Illinois, USA). On the desktop beamline (DTB), the beam stop can be translated between 10 mm to 45 mm from the phi-axis (sample position) to prevent the CCD detector from the primary X-ray beam. Therefore, the GIXRD sample holder must be less than 20 mm in width.

The sample holder was made from a plastic plate with dimensions of 1.5×3.0 $cm^2$. One side of the sample holder is a magnet. Thus, this modified sample holder can be mounted on the goniometer for grazing experiments. Taking the advantage of accurate controlling of a high precision phi-axis of the MarDTB goniometer system, thus, the sample can be tilted/rotated to adjust the angle of incidence between 0° to 360°

with accuracy 0.002°. Thus, diffraction measurements with geometry is doable without any difficulties.

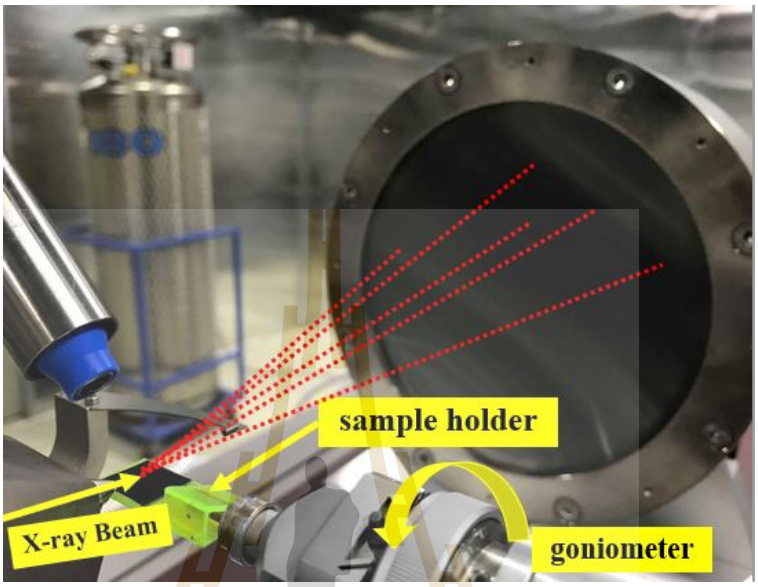


**Figure 3.5** Photo of the experimental station of the BL7.2W:MX beamline with modification of sample holder for GIXRD measurement.

## 3.4 The GIXRD experimental station

### 3.4.1 The alignment of X-ray beam

Before the X- ray beam produced from SWLS enters the DCM, the vertical beam position shell be adjusted to provide the maximum photon flux measured by position monitor (VBPM). Then the maximization of the photon flux after the DCM carried out by making both crystals to be parallel. After that, the photon energy is calibrated by using a suitable standard foil which available at the beamline. The flux of photon energy was measured before entering the beam shaping section. The alignment of the X-ray beam by optimization and calibration of DCM to get the optimum flux for

the measurements. Adjusting the size of the incident beam at the sample position is very important to achieve the optimum conditions. The X-ray beam must be kept as small as possible to preserve the intrinsically sharp diffraction features from the sample (Colin Nave, 2014). The X-ray beam size at the beamline is adjusted by two-pairs slits of the collimator component on the MarDTB system by driving horizontal and vertical translation motors.

### 3.4.2 Selection of sample to detector distance and the X-ray energy

Figure 3.6 represents a schematic of X-ray diffraction. It can be seen that the diffraction angle (θ) depends on diffraction plane of the sample (m) and the sample to detector distance (S), thus, the diffraction angle can be calculated from

$$\theta = \arctan\left(\frac{m}{S}\right) \tag{3.1}$$

According to the set up available at the beamline (S can be move from 45 to 390 mm), the minimum and maximum of diffraction angle are 11.94 and 61.38 degree respectively. Furthermore, the number of diffraction peaks and appropriate exposure time depend on the sample materials and the distance between the sample to detector. Thus, optimization of the sample to detector distance must be considered for different sample materials. In addition, X-ray energy can be selected by the double-crystal monochromator (DCM). This provides the flexibility in choosing appropriate photon energy for various types of experiments. Considering Bragg' s law (2.1), if the photon energy is changed, the diffraction angle (2θ) are calculated from

$$\frac{\sin\theta_1}{\lambda_1} = \frac{\sin\theta_2}{\lambda_2} \tag{3.2}$$

$$\theta_2 = \sin^{-1}\left(\frac{\sin\theta_2\lambda_1}{\lambda_2}\right) \tag{3.3}$$

Where $\theta_1$ and $\theta_2$ are incident angle of X-ray beam of the monochromatic wavelength $\lambda_1$ and $\lambda_2$ respectively. Thus, from eq. (3.3), the limitation of the diffraction angle ($2\theta$) that can be detected at the beamline are summarized in table 3.

### 3.4.3 Pattern alignment and calibration of sample to detector distance

To convert from a 2D GIXRD image to a 1D 2-Theta diffraction curve, it is necessary to know the distance from pixel position on the detector pixel to the position of the primary beam. But the primary beam is blocked by a beam stop to prevent the detector that may be damaged by the high intensity of the primary beam. This prevents us directly observe the position of the primary beam. Thus, measurements of a standard that has a circular diffraction pattern which makes it possible to indicate the primary beam from the center of the circle. The center of a circular diffraction pattern which is the primary beam position can be determined by using SAXIT programs. In addition, measurements of the standard can also be used to calibrate the sample to detector distance (S distance in figure 3.6).

### 3.4.4 GIXRD sample alignment

Before GIXRD measurements, the sample holder has to be adjusted appropriately to the pin hole, and vertically aligned and further checked by exposing with a burn paper. The burn paper should be located on the support that has the same thickness as the sample thickness. Phi-axis of MarDTB goniometer system should be slightly tilted. According to the calibrated sample to detector distance, the X-ray beam should be incident on the paper burn at the same position of the standard that is used for calibrating of sample to detector distance. Figure 3.7 shows a schematic of the position of X-ray beam incident on the paper burn with different positions. As described before, the peak positions of XRD data are determined by a sample to detector distance.

Misalignment of the sample holder causes a small amount of error in the peak positions. For instance, if the X-rays beam is incident at the end of the sample (close to detector), the GIXRD pattern shows the peak shift to a higher 2-theta angle. Troubleshooting of this misalignment can be done by slightly move the sample holder down and checking by expose the X-ray again until the X-ray beam is incident on the position of the standard calibration SSD. When the alignment of sample is done, the sample holder should be move up with the distance equal to the thickness of the paper burn. Appropriate exposure time for samples should be tried.

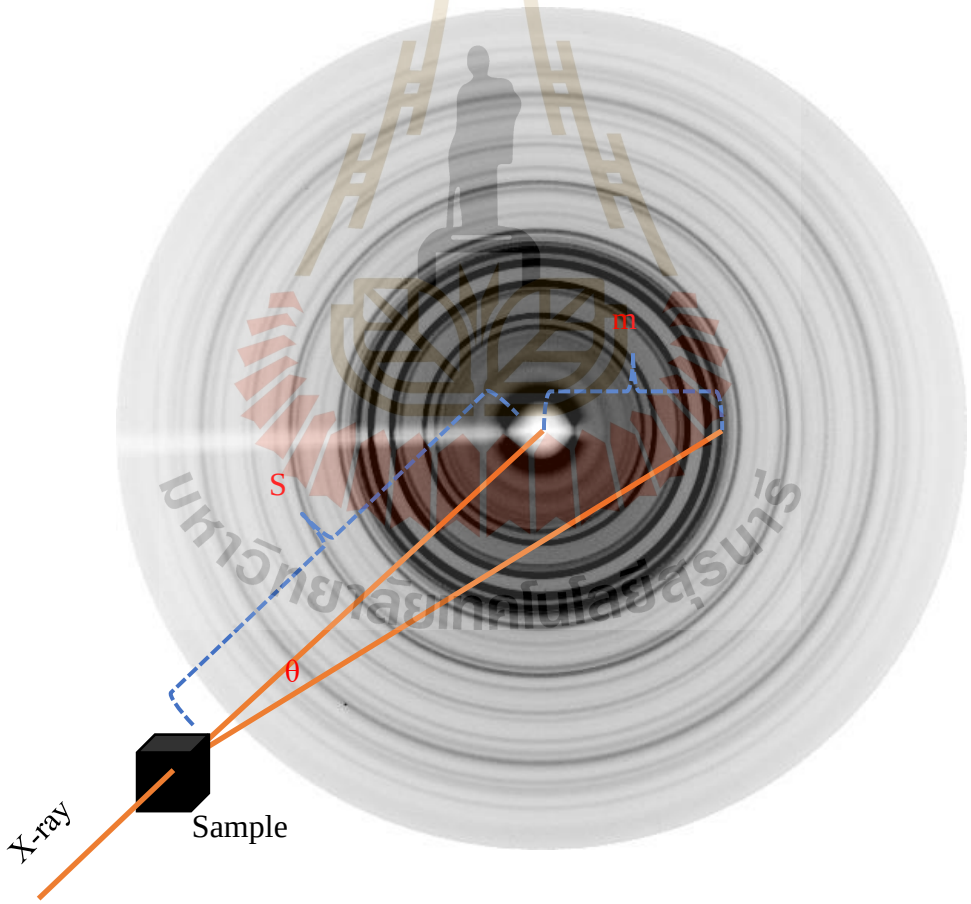


**Figure 3.6** Schematic of diffraction pattern of X-rays from a sample.

**Table 3** Diffraction angle at sample to detector distance 45 and 390 mm.

| Energy range (keV) | Sample-detector distance 45 mm. | Sample-detector distance 390 mm. |
|---|---|---|
| | Maximum 2θ (degree) at CuKα (1.54Å) | Maximum 2θ (degree) at CuKα (1.54Å) |
| 7 | 52.6 | 60 |
| 8 | 60.8 | 69 |
| 9 | 69.4 | 78 |
| 10 | 78.5 | 86 |
| 11 | 88.2 | 95 |
| 12 | 98.8 | 104 |
| 13 | 110.7 | 112 |
| 14 | 124.8 | 12.1 |
| 15 | >124 | 130 |
| 16 | >124 | 139 |
| 17 | >124 | 147 |
| 18 | >124 | 156 |

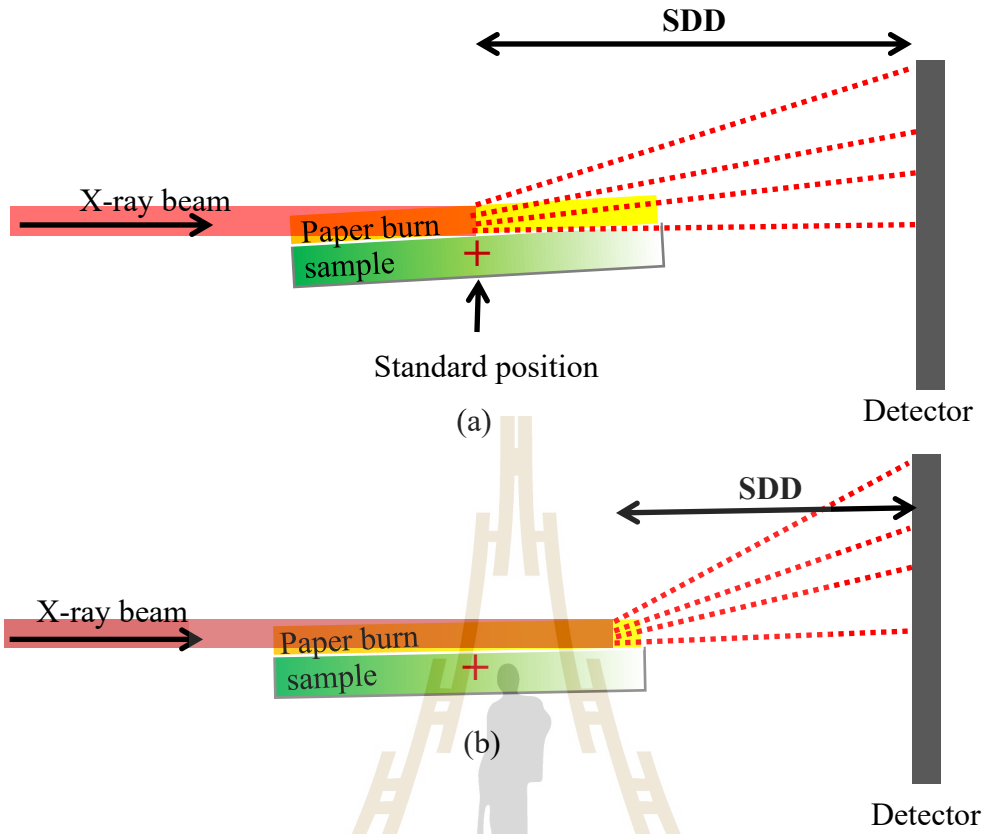


**Figure 3.7** A schematic of GIXRD sample holder alignment with X-ray beam (a) Alignment at the same position of standard calibration SDD and (b) Misalignment from the position of standard calibration SDD.

### 3.4.5 Commissioning GIXRD measurement system

The commissioning of the GIXRD set up was carried out on a 4-bromo benzoic acid, germanium antimony tellurium (GST) and aluminum doped zinc oxide (AZO) thin films. The 4-bromo benzoic acid was used as a calibration standard to determine the accurate distance between the sample and detector. The diffraction images were collected using a monochromatic X-ray beam with a wavelength of 1.291 Å (9,600 eV), calibrated from the K absorption edge close to the energy required. Grazing incidence angle was fixed at 1.0° for GST thin film and 0.6° for AZO thin film, respectively. The distance between the sample to the detector was fixed at 45 mm and both thin films were taken with a collection time of 2 min, the commissioning results and systematic errors arising from the measurement were further analyzed and discussed in the next chapter.

## 3.5 GIXRD in-situ cell

XRD is one of the most commonly applied techniques to provide information on the crystalline phases. However, the structure of materials can be changed during reaction by heating, annealing, or cooling steps. This may induce changes in the properties of materials i.e. dielectric properties depend strongly on microstructure (Xinyi *et al.*, 2012). Thus, in-situ XRD has been developed and utilized for investigations of materials as a real-time (Clausen *et al.*, 1991; Moury *et al.*, 2015) to understand the fundamental under the process of reaction. In this work, the GIXRD in-situ cell is developed, which is the instrument used for real-time characterization of thin films. The design and construction of a GIXRD in-situ cell are described below.

A schematic of a GIXRD in-situ cell is given in figure 3.8. The main chamber of a GIXRD in-situ cell is made of a block of stainless steel with two windows for the incoming, and diffracted X-ray beams. The top of the main chamber is connected with a motorize stage to align the cell in the X-ray beam (vertical adjustment) a lock cap is installed at one side of the main chamber to hold a GIXRD in-situ cell with the goniometer head at the exit of the X-ray beam. The sample holder is in the main chamber. The sample holder is designed to retain thin film samples with 1×1 $cm^2$ in dimensions. This holder is connected with the graphite plate heater. This heater is covered with the ceramic plate to protect the heating system from short circuit and connected with thermocouple for monitoring the sample temperature. A micrometer head is located under the sample holder, to adjustment the grazing angle between X-rays and the sample. The bottom of the main chamber is connected with the compartment with gas inlet/outlet, this prevents the main cell body from heating up, as shown in figure 3.9.

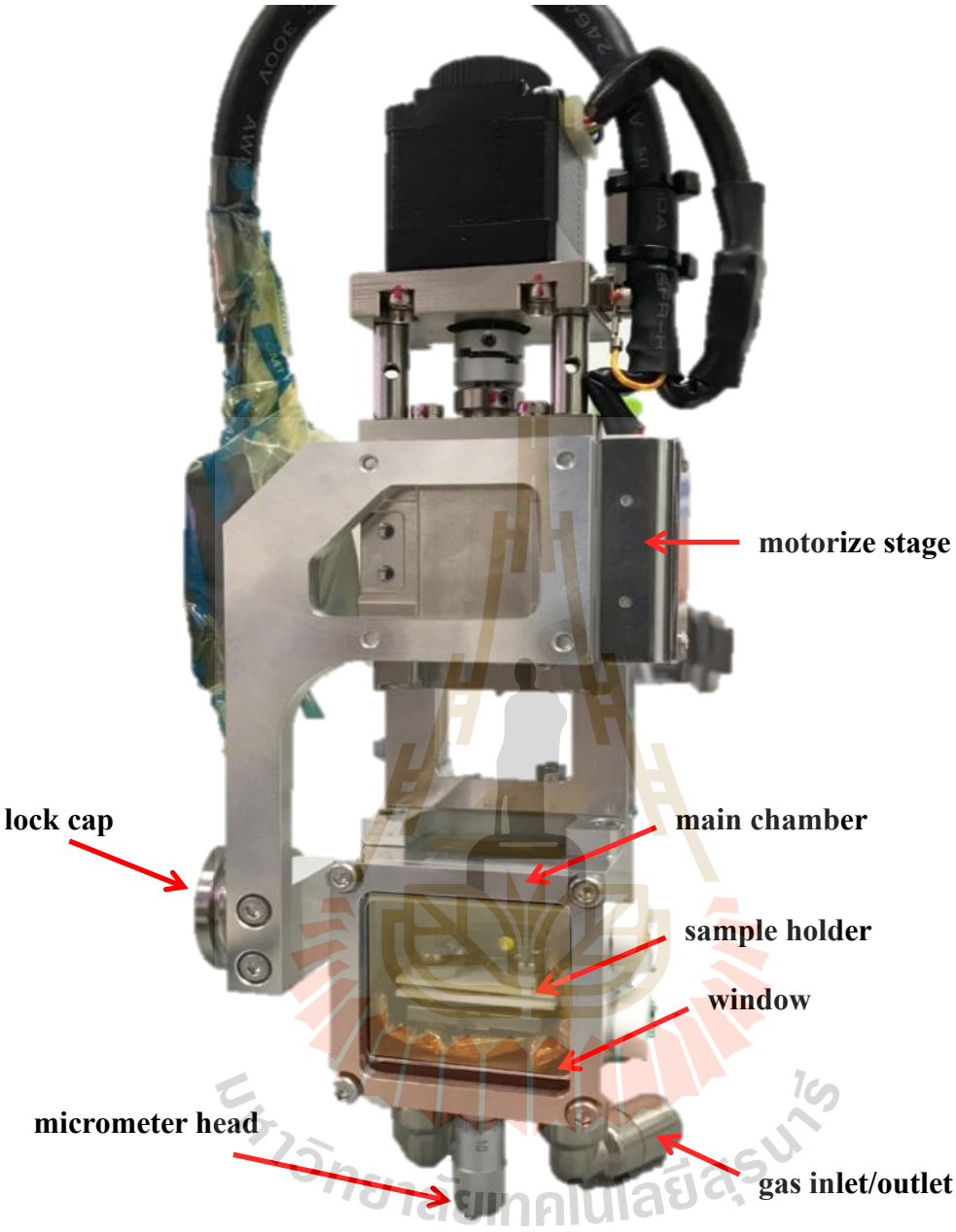


**Figure 3.8** Schematic of GIXRD in-situ cell.

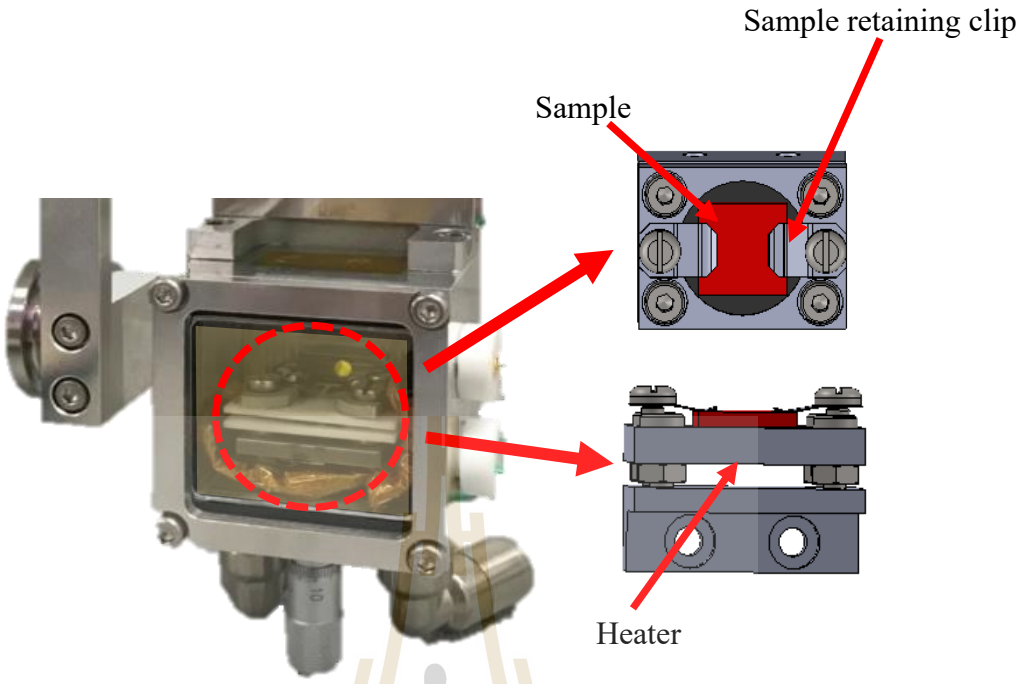


**Figure 3.9** Front view of GIXRD in-situ cell

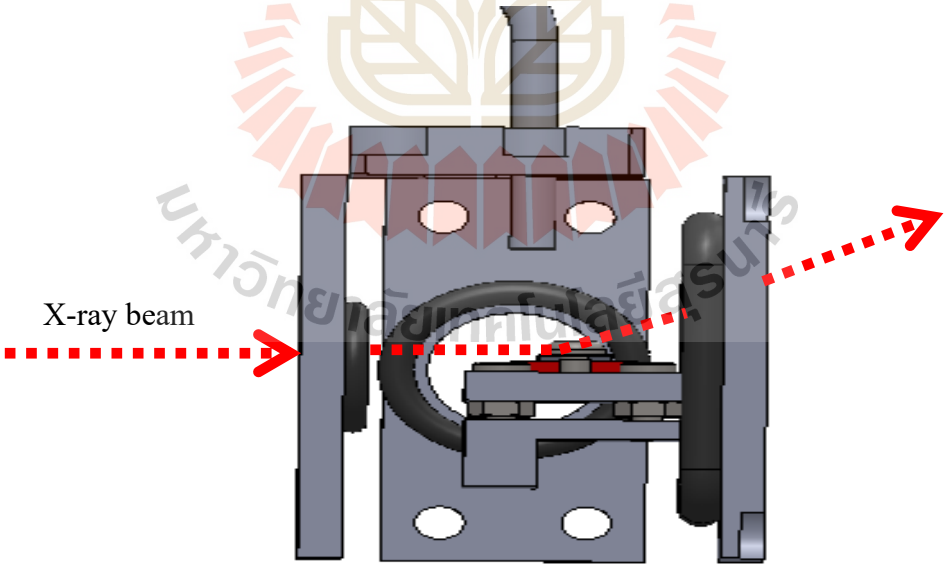


**Figure 3.10** Side view of main chamber GIXRD in-situ cell.

# CHEPTER IV

# RESULTS AND DISCUSSIONS

In this thesis work, the development of the GIXRD technique was carried out at the BL7.2W: MX beamline. The photon flux energy and optimization of the beam size for GIXRD measurement are reported. The obtained data were analyzed. The systematic error arising from the GIXRD measurements and the commissioning results from GIXRD experimental station of BL7.2 W: MX beamline are also reported and discussed in this chapter.

## 4.1 Photon flux, beam size and optimization of SDD

The actual photon flux measured before entering the beam shaping slits of the XRD set up is shown in figure 4.1. It is clearly shown that the photon flux from 7 to 18keV range is in the order of $10^{10}$ photons/s@100mA, which is more than sufficient for general XRD measurements. The photon flux is varied with photon energy and maximum at about 8 keV. Figure 4.2 illustrated the shape of beam size observed by CCD microscope with adjusted two-pair slits. For GIXRD measurement the beam size was reduced down to 1 x 0.025 mm2 (H x V) (figure 4.2d) and further checked by exposure with burn paper.

Figure 4.3 shows the diffraction image of 4-bromo benzoic acid obtained by transmission mode with two different distance of sample to detector. The closer to the

sample, the more diffraction peaks are collected at the detector. Figure 4.4 shows the position of X-ray beam expose on paper burn by rotating the sample holder of GIXRD

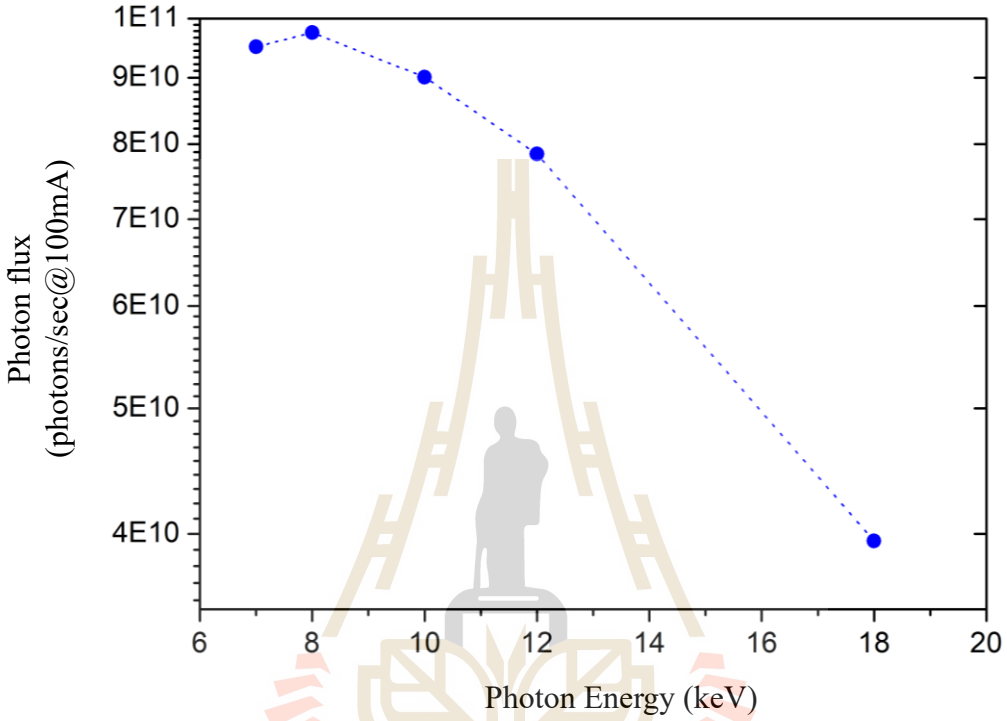


**Figure 4.1** Measured photon flux before entering the beam shaping slits of the XRD measurement system.

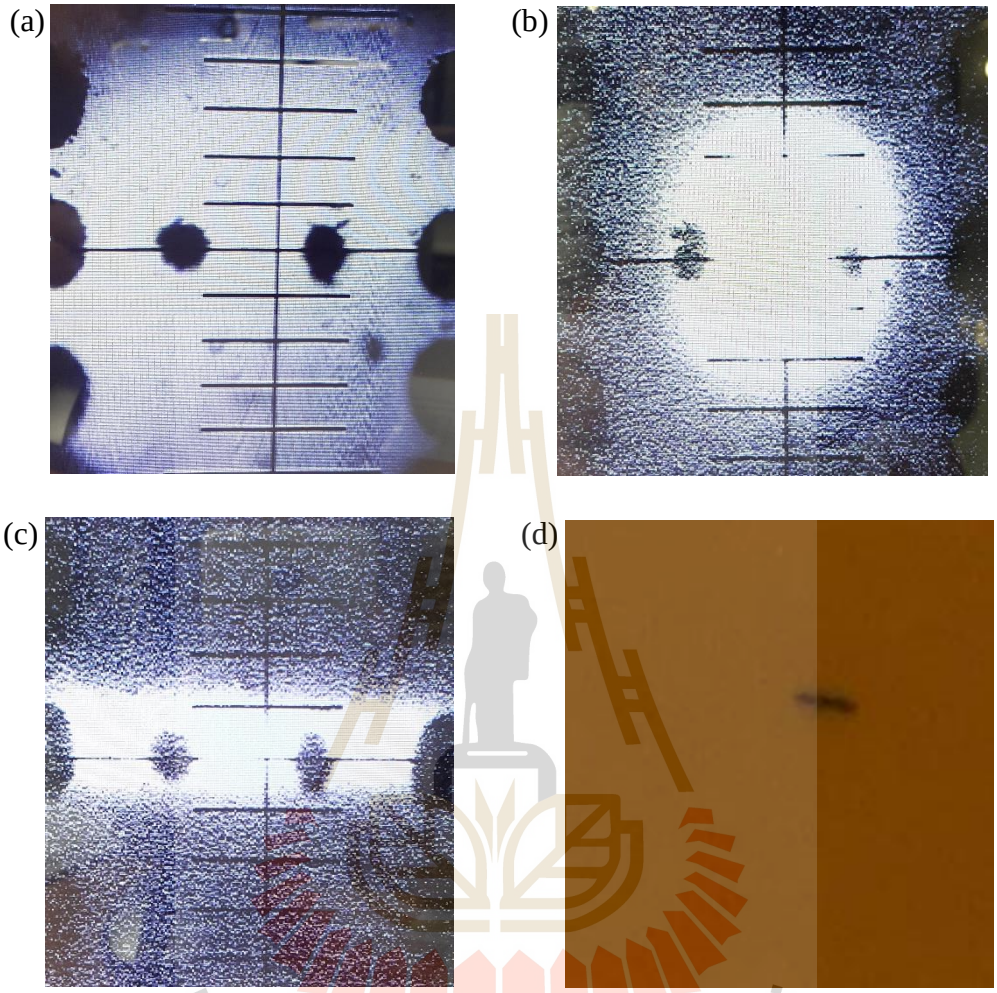


**Figure 4.2** Photo illustrating of beam shapping by adjusting two-pair slits of collimator of the MarDTB system (a) full beam 4×4(H×V) $mm^2$ (b) 0.3×0.3(H×V) $mm^2$ (c) 4×0.025(H×V) $mm^2$ and (d) X-ray exposing with paper burn 1×0.025(H×V) $mm^2$.

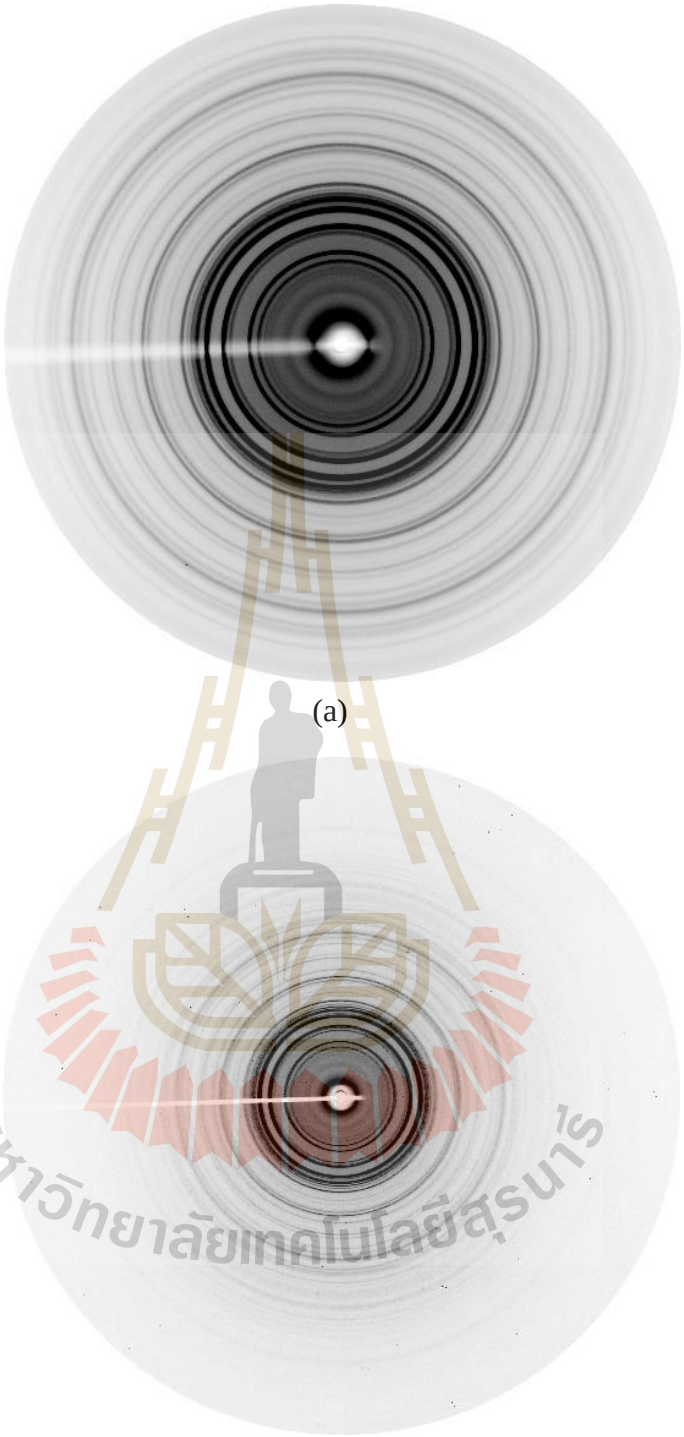

(a)

(b)

**Figure 4.3** 2D diffraction images of 4-bromo benzoic acid with different distances of sample to detector (a) 80 cm. and (b) 45 cm.

**Figure 4.4** The position of X-ray beam exposing on the burn paper.

## 4.2 Systematic error from GIXRD measurement

Figure 4.5 shows a GIXRD image of AZO thin film with misalignment. GIXRD image appeared as broadening peak and some diffracted beam are appeared at a lower of GIXRD image pattern, this suggests that the X-ray beam is incident on the end of the sample. Figure 4.6 represents GIXRD pattern of the AZO thin film compared with a reference pattern of ZnO from JCPDS #36-1451. The 2-theta peak of AZO GIXRD pattern shifted toward to a higher angle compared with the reference. Normally, XRD data are compared to reference patterns to determine what phases are present. The positions and intensity of the reference should match the data. The sample holder displacement is a systematic peak position error due to misalignment of the GIXRD sample holder. As mention before in chapter III, the diffraction angles ($2\theta$) are dependent on diffraction planes of the sample and sample to detector distance. Thus, the GIXRD sample holder should be aligned by exposing the X-ray beam with incident the burn paper in the same position of a standard that was used for SDD calibration.

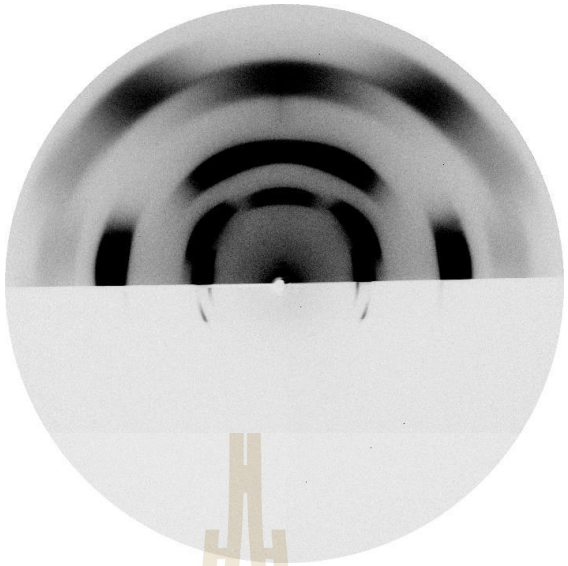

**Figure 4.5** A GIXRD image of AZO with misalignment of the sample holder.

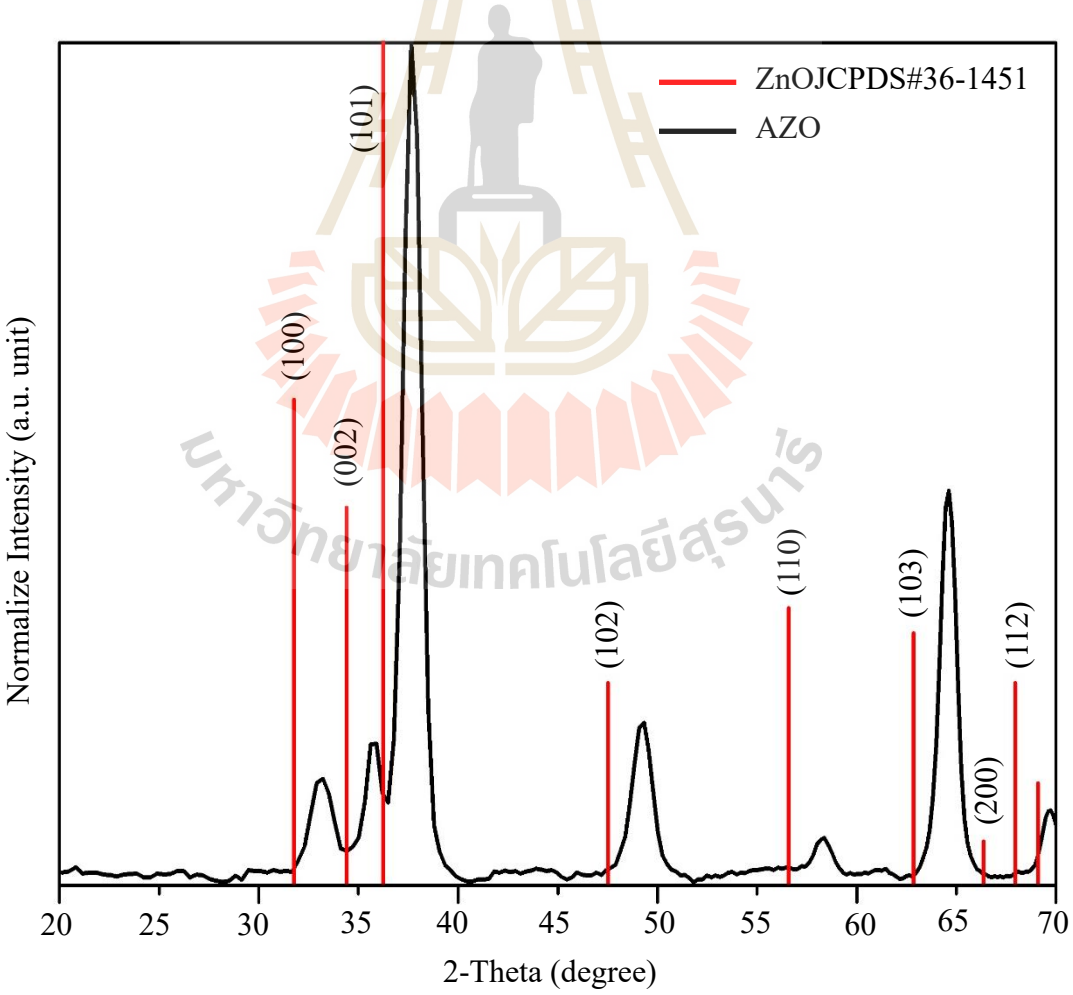


**Figure 4.6** A GIXRD pattern of AZO compared with a reference pattern of ZnO.

## 4.3 Commissioning results

Figure 4.7(a) and (b) show X-ray diffraction images taken from germanium antimony tellurium (GTS) and aluminium doped zinc oxide (AZO) thin films, respectively, synchrotron X-ray with a wavelength of 1.291Å (9600eV). The full Debye ring in figure 4.7(a) indicates that the X-ray beam is incident on the sample with tiny crystals in all orientations, implying that the sample has a perfect polycrystalline texture (Widjonarko 2006). Whereas the diffraction image taken from the AZO thin film appears as a partial ring, as shows in figure 4.7(b). Thus, this AZO film is not polycrystalline. The film was grown with preferred orientations. With a 2D detector used at the beamline, one can collect diffracted beams in 2 dimensions. The X-ray diffraction image of AZO film was converted to one-dimensional pattern by using SAXIT program (Rugmai *et al.*, 2013). Figure 4.7(c) illustrates a one-dimensional diffraction pattern of AZO film. It is clearly seen by comparing data from the beamline and a conventional system. The diffraction beams observed at the beamline results from the diffraction planes (100), (002), (110), (102), (110), (103) and (112) whereas a conventional laboratory GIXRD system only the diffraction planes of (002) and (103) are observed.

The high intensity of synchrotron X-ray requires a short data collection time. The diffraction images/patterns in figure 4.7 were taken with collection time of 2 and 45 min at the synchrotron beamline and conventional GIXRD laboratory system, respectively. In addition to the advantage of a short data taking time, the synchrotron GIXRD can be carried with any X-ray wavelength from 7 to 18 keV, thus depending on specific requirements suitable for different sample materials.

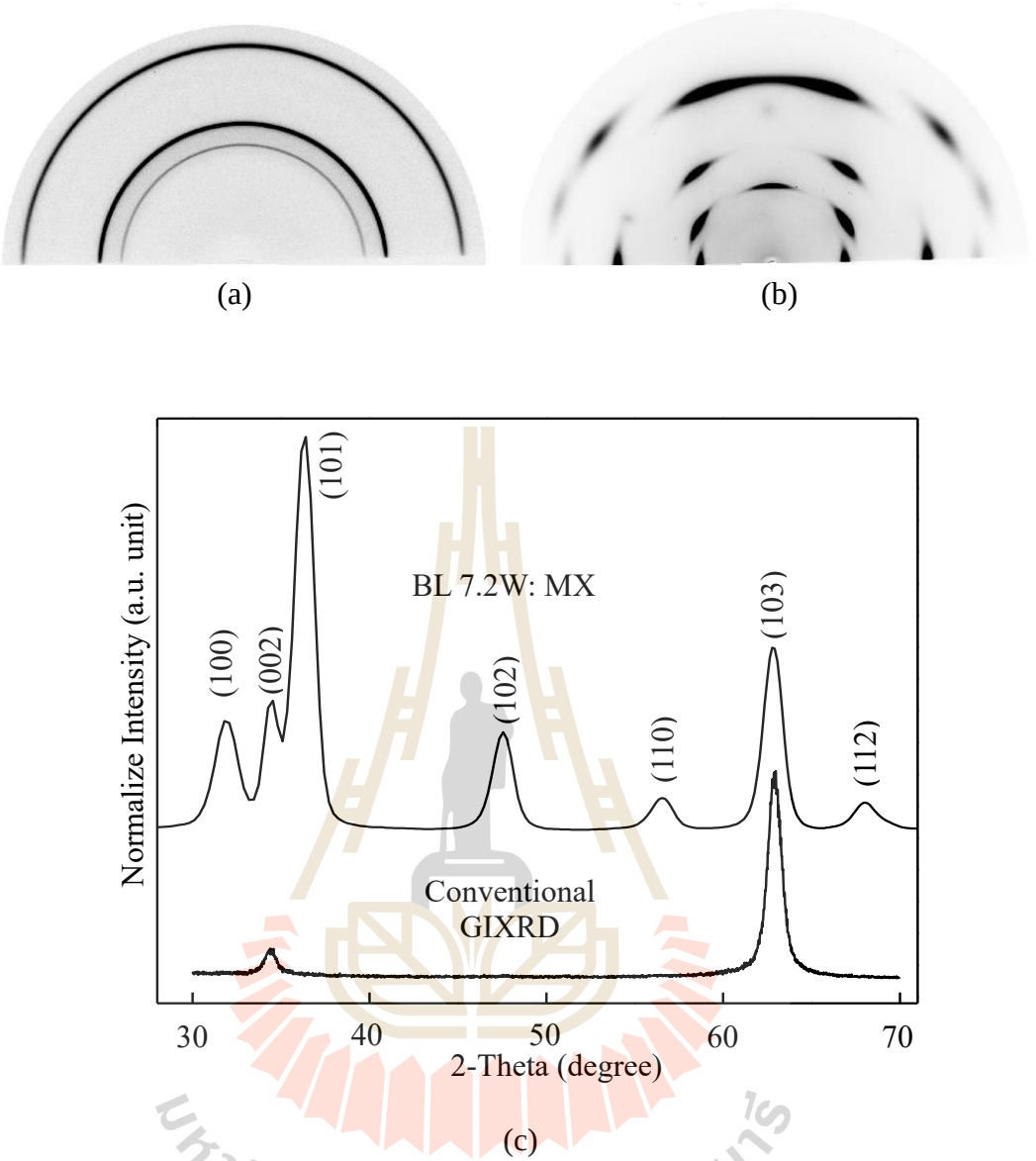


**Figure 4.7** 2D GIXRD diffraction images of (a) GTS, (b) AZO thin films and (c) GIXRD patterns of AZO film measured at the BL7.2W:MX beamline (top) and conventional GIXRD system (bottom).

## 4.4 GIXRD of AZO thin film

In this work, The AZO thin films were deposited on silicon wafer (001) substrates prepared by pulsed DC magnetron sputtering, with different incidence angle. GIXRD was employed to study AZO. It was known that two-dimensional X-ray diffraction systems have many advantages over conventional one-dimensional diffraction systems (Bob *et al.*, 2003). The orientation distribution of several crystallographic planes over a range of angles of AZO thin film can be measured simultaneously.

GIXRD measurements of AZO thin film have been carried out at BL7.2 W: MX beamline at SLRI. The X-ray energy was fixed at 9.6 keV ($\lambda$ = 1.291 Å) and the measurements were carried out in a reflection mode with grazing angle varying from 0.5 to 10 degrees to vary the interaction of each penetration depth on the thin films. The data were collected by a Mar165 CCD detector system (Rayonix LLC, Evanston, Illinois, USA) at a distance of 47 mm from the sample, which was calibrated by 4-bromo benzoic acid powder in transmission mode. The obtained 2D diffraction images were processed with 2D image processing computer programs, e.g. SAXSIT which is developed for analyses of small angle X-ray scattering data.

(a) (b)

**Figure 4.8** 2D GIXRD diffraction images of AZO dense films with fixed grazing angle of (a) 0.5° and (b) 10°

Figure 4.8 illustrates the diffraction images taken from dense AZO thin films with fixed incidence angle at (a) 0.5° and (b) 10°. The diffraction image appears as a partial Debye ring, implying that the films is not polycrystalline texture. The film was grown with a preferred orientation. In literatures, the AZO thin film that prepared by using the magnetron sputtering technique normally are shows only a few peaks ((002), (100), (101) and (103) etc.) in the XRD results as reported by (Wu *et al.*, 2012; Li *et al.*, 2013; Sun *et al.*, 2016).

All diffraction images were processed to 2-theta curve with varying the grazing angle from 0.5° to 10°, as shown in figure 4.9. The results show that the AZO dense films comprise with the diffraction planes of hexagonal wurtzite structure of ZnO with the same diffraction planes of (100), (002), (110), (102), (110), (103) and (112) (usually appears in conventional powder XRD pattern) in every incidence angle that was tilted. The width of 2-theta of the AZO dense films tend to exhibit a broad peak when the incidence of angle decreases.

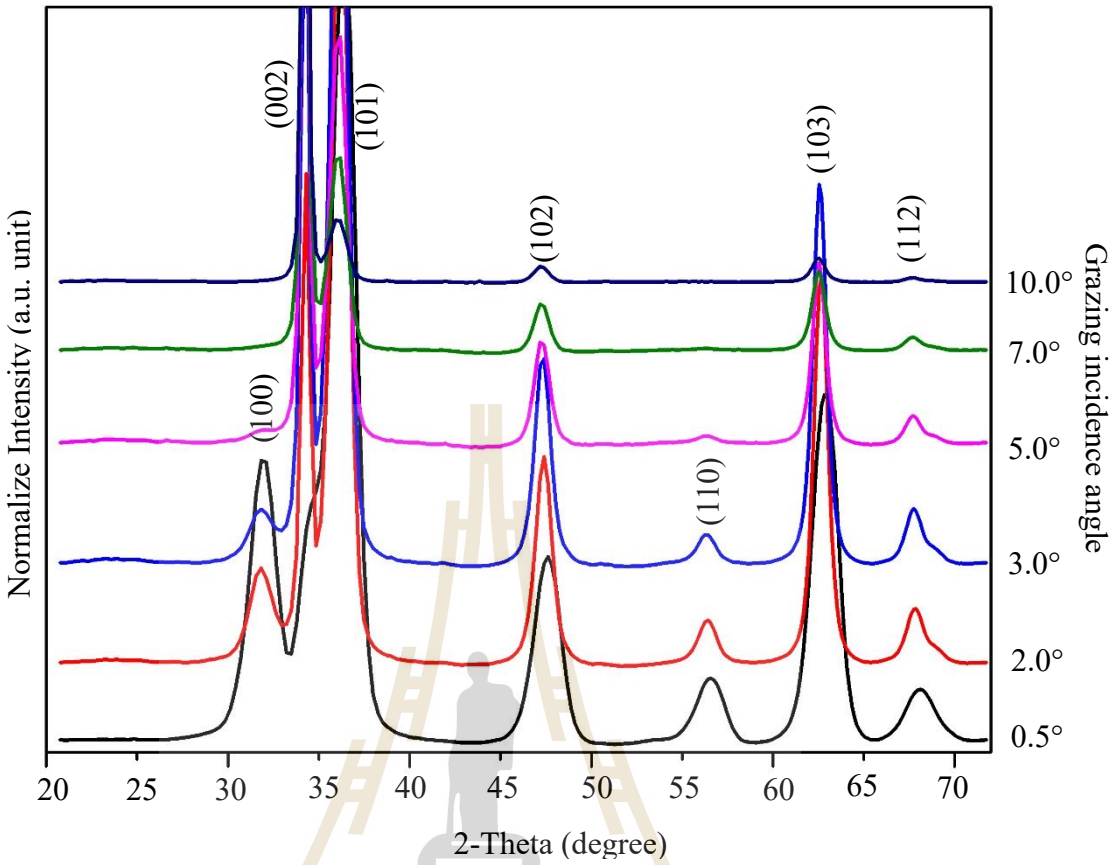


**Figure 4.9** GIXRD results of AZO dense film with different grazing angles from 0.5° to 10°

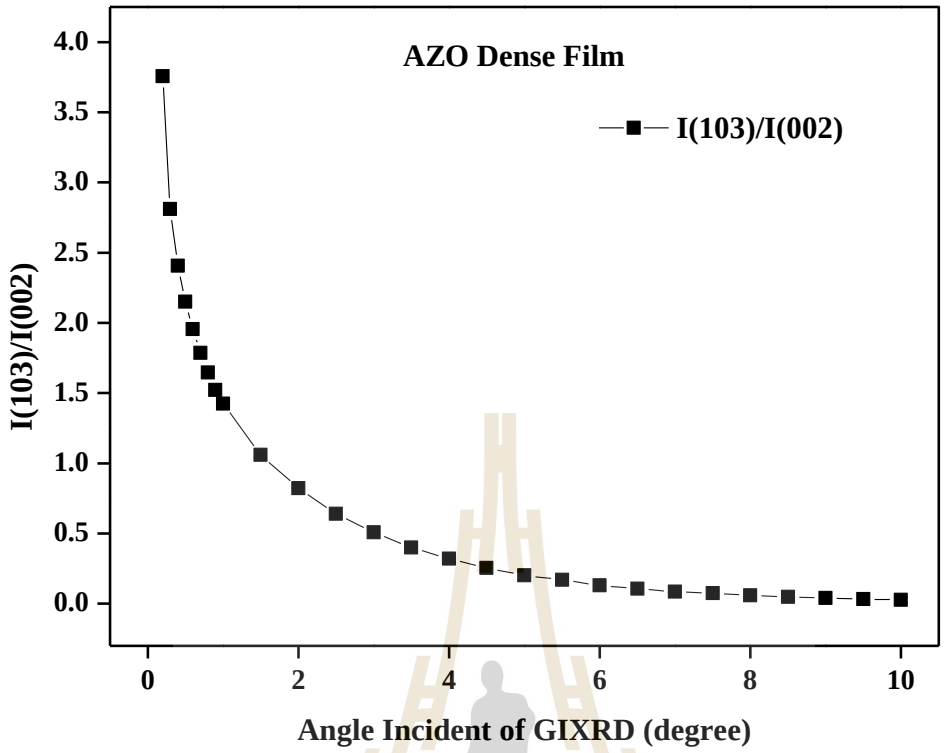


**Figure 4.10** The ratio of I(103)/I(002) of AZO dense films.

Figure 4.10 shows the ratio of the intensity that were collected by CCD detector of (103) and (002) peak. The results are similar to Wang's results (Wang *et al.*, 2012) that are reported before. The ratio decreased dramatically when the sample was tilted from 0.5° until around 3° (incidence of angle) and slightly drops until the incidence angle was 10°. This indicates that the sample are different between the bottom and the surface layer.

As can be seen in figure 4.7, the orientation distribution of crystallites in the AZO thin film is not perfectly random. The observed azimuth angle values of (002) and (103) peaks are showed in table 4. From the results, the azimuth angle of (002) is not changed when the incidence angle was increased while the azimuth angle of (103) variated from bottom to surface about 10 degrees. Thus, the extent of (103) peak is resulting from the growth mechanism of the sample not from the error of measurement.

**Table 4** FWHM of azimuth angle of (002) and (103) peaks.

| Grazing Incident Angle (degree) | Azimuthal angle of (002) (degree) | | Azimuthal angle of (103) (degree) | | | |
|---|---|---|---|---|---|---|
| | Dense Film | Columnar Film | Dense Film | | Columnar Film | |
| 0.5 | 88.49 | 89.37 | 71.37 | 105.97 | 70.69 | 106.68 |
| 3.0 | 88.49 | 89.40 | 67.31 | 110.07 | 67.28 | 111.48 |
| 5.0 | 88.56 | 89.39 | 65.04 | 112.37 | 64.91 | 113.83 |
| 7.0 | 88.57 | 89.38 | 63.11 | 114.37 | 62.83 | 115.88 |
| 10.0 | 88.58 | 89.45 | 60.40 | 117.07 | 60.51 | 118.23 |

## 4.5 XRD and GIXRD of MnBi

MnBi powder was prepared by sintering method. Mn99% (149μm) and Bi99.5% (400μm) powder were mixed in crucible and then heated to 300°C in vacuum chamber under $5\times10^{-7}$ mbar base pressure. The sample was annealed 6 hr. at 300°C and then cooled down to room temperature. The structure of sample was characterized by XRD with two different geometry, transmission geometry and GIXRD geometry with grazing angle of 3°. The X-ray energy was fixed at 12.658 keV ($\lambda = 0.980$ Å).

Figure 4.11 demonstrates 2D diffraction images of MnBi taken with collection time of 5 min. (a) transmission XRD geometry and (b) GIXRD geometry, respectively. The results showing that, MnBi are polycrystalline (Widjonarko 2006). A 2D diffraction images were converted to one- dimensional pattern by using SAXIT (Rugmai *et al.*, 2013) program. Figure 4.12 represents one-dimension of MnBi powder measured with transmission XRD and GIXRD respectively. It is clearly seen that the MnBi phase can be detected when using GIXRD measurement compared with transmission XRD measurement. This implies that this MnBi powder consists of an Mn core with MnBi shell. Since GIXRD presents more details of surface information than

XRD and smaller grazing angle guarantees more details of surface information than the larger angle (Nauera *et al.*, 2005).

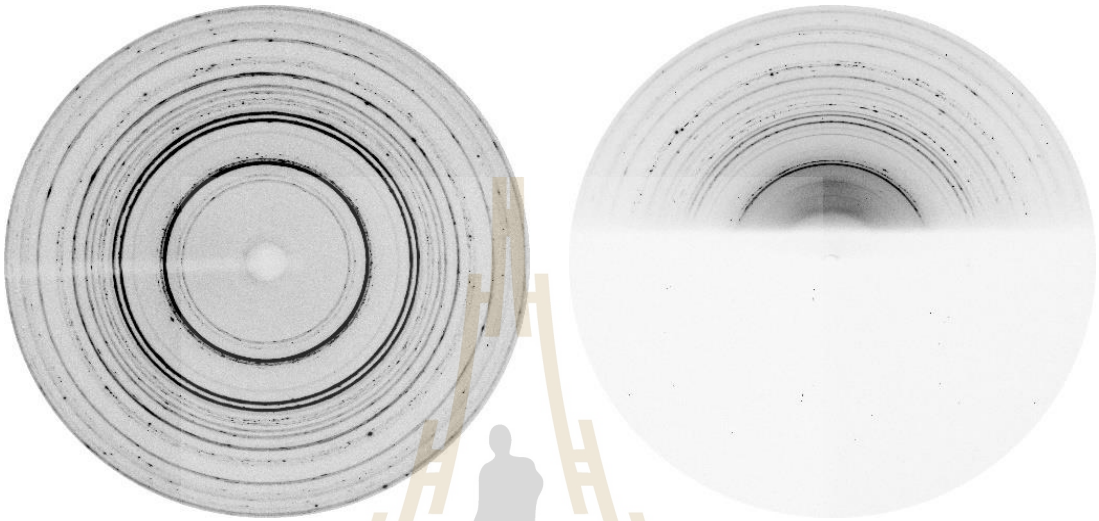

(a) (b)

**Figure 4.11** 2D diffraction image of MnBi (a) transmission XRD geometry (b) GIXRD geometry with grazing angle of 3°.

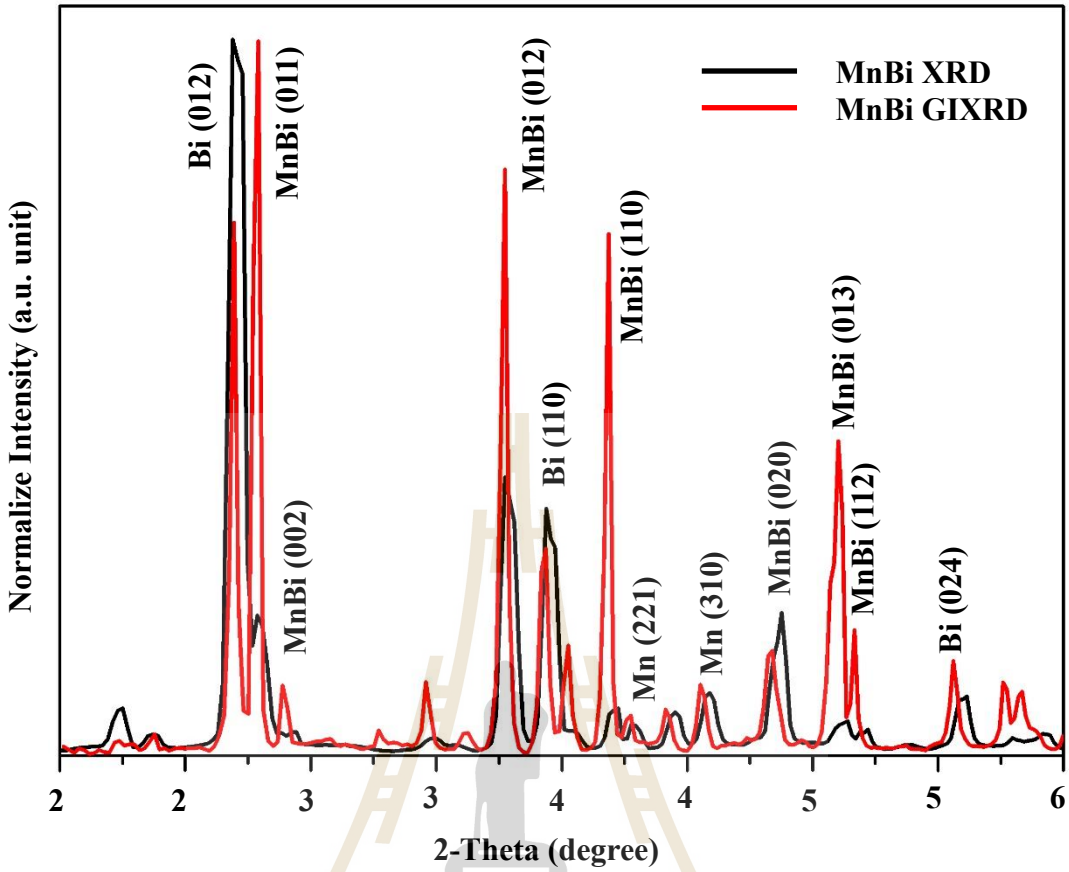


**Figure 4.12** XRD and GIXRD result of MnBi powder was carried out with grazing angle of 3°.

# CHEPTER V

# CONCLUSIONS

This thesis work focused on the development of a grazing incidence X-ray diffraction (GIXRD) technique at the BL7.2W: MX beamline of the Synchrotron Light Research Institute (SLRI). Aluminium-doped zinc oxide films and manganese bismuth powder were used as the materials for commissioning the measurement system. It was demonstrated that Synchrotron X-rays at the BL7.2W: MX beamline of SLRI can be used for GIXRD measurements. The beamline utilizes X-rays produced from a 6.5T superconducting wavelength shifter. A double-crystal monochromator is used to choose X-ray photon energy covering from 7 to 18 KeV. The vertical beam size on the sample was found to be essential for GIXRD measurements since the required grazing angle must be as small as 0.1 degree for ultra-thin film samples. The larger vertical beam, the larger effective beam size on the sample resulting in a larger dispersion of the distance between the sample to detector and, in turn, giving broad diffraction beams. It was found that the practical vertical beam size is 20 microns while the horizontal can be as big as 1.0 mm to provide sufficiently high photon flux.

The advantages of synchrotron GIXRD at SLRI over conventional XRD systems have been demonstrated. Firstly, synchrotron X-rays at the BL7.2W is more intense than X-rays from laboratory sources and thus shortening time for the measurements when using synchrotron X-rays. It was shown that a 45-min measurement using laboratory X-ray could be reduced to a 2-min when using the

BL7.2W measurement system. Secondly, synchrotron X-rays at the BL7.2W covers a wide range of photon energy (or wavelength), from 7 to 18 keV. Thus, GIXRD measurements can be done with tunable X-rays by using the monochromator to select the X-rays with required photon energy or wavelength. This provides the possibility to choose a proper photon energy, particularly, to avoid X-ray absorption by the elements in the samples. Last but not least, the experimental station for this work employs a 2-dimentional CCD detector. This allow diffracted beams with a certain solid angle, depending the distance between sample to detector, to be simultaneously measured and thus short data acquisition time is required for the measurements. In addition, the CCD detector can detect some diffracted beams that cannot be measured by a 1-dimentional detector as it was found for the case of the AZO films. Therefore, the CCD detector allows more types of materials to be investigated by the diffraction technique.

Furthermore, an in-situ cell was designed and constructed for future GIXRD measurements. The in-situ cell allows GIXRD measurements to be carried out with the samples in controlled conditions. The samples might be heated up about 600 degree Celsius, and the ambient gas species can be controlled by feeding required gases.

# REFERENCES

# REFERENCES


Bob, B. H., Uwe P. and Kingsley, L. S. Comparison between conventional and two dimentional XRD (2003). **XRD International Centre for Diffraction Data 2003, Advances in X-ray Analysis** 46: 37.

Catlow, C. R. A. and Greaves, G. N. (1991). Application of synchrotron radiation (29 West 35th Street, New York, NY 10001-2291) ISBN 0-216-92677-7.

Colombi, P., Zanola, P., Bontempi, E., Roberti, R., Gelfi, M. and Depero, L. E. (2006). Grazing-incidence X-ray diffraction for depth profiling of polycrystalline layers. **J. Appl. Cryst**. 39: 176.

Klysubun, W. , Sophon, M. , Phanak, M. , Deethae, N. , Wongprachanukul, N. , Suthummapiwat, A. , Cherdchoo, P. and Songsiriritthigul, P. ( 2010) . Development of a hard X-ray beamline for macromolecular crystallography at the Siam Photon Laboratory. **The Fifth Asia Oceania Forum for Synchrotron Radiation Research** (Pohang: POSCO International Center).

Kriegner, D., Matěj, Z., Kužel, R. and Holý, V. (2015). Powder diffraction in Bragg–Brentano geometry with straight linear detectors. **J. Appl. Cryst**. 48: 613.

Li, X., Wang, Y., Liu, W., Jiang G. and Zhu, C. (2012). Study of oxygen vacancies' influence on the lattice parameter in ZnO thin film. **Materials Letters** 85: 25.

Ly, V., Wu, X., Smillie, L., Shoji, T., Kato, A., Manabe, A. and Suzuki, K. (2014). Low-temperature phase MnBi compound: A potential candidate for rare-earth free permanent magnets. **J. Alloys Comp.** 615: 285-290


.

Marra, W. C., Eisenberger, P. and Cho, A. Y. (1997). X ray total external reflection–Bragg diffraction: A structural study of the GaAsAl interface. **J. Appl. Phys** 50: 692.

Mikio, K. and Kunio, W. (1997). Magnetic properties of MnBi particles **J. Appl. Phys.** 48: 4640-4642.

Moon, K., W., Jeon, K. W., Kang, M., Kang, M. K., Byun, Y., Kim, J. B., Kim, H. and Kim, J. (2014). Synthesis and Magnetic Properties of MnBi (LTP) Magnets with High-Energy Product. **IEEE Trans Magn.** 50: 2103804–2103804

Nauera, M., Ernst, K., Kauteka, W. and Neumann-Spallartb, M. (2005). Depth profile characterization of electrodeposited multi-thin-film structures by low angle of incidence X-ray diffractometry **Thin Solid Films** 489: 86–93

Neuschitzer, M., Moser, A., Neuhold, A., Kraxner, J., Stadlober, B., Oehzelt, M., Salzmann, I., Resel, R. and Novak, J. (2012). Grazing-incidence in-plane X-ray diffraction on ultra-thin organic films using standard laboratory equipment. **J. Appl. Cryst**. 45: 367.

Ning, Z. Y., Cheng, S. H., Ge, S. B., Chao, Y., Gang, Z. Q., Zhang, Y. X. and Liu, Z. G. (1997). Preparation and characterization of ZnO: A1 films by pulsed laser deposition. **Thin Solid Films** 307: 50.

Ohyama, M., Kozuka, H. and Yoko, T. (1997). Sol-gel preparation of ZnO films with extremely preferred orientation along (002) plane from zinc acetate solution. **Thin Solid Films** 306: 78.

Rugmai, S. and Soontaranon, S. SAXSIT Manual (2013) (Nakhon Ratchasima: Siam Photon Laboratory) ISBN 978-616-120274-3.

Saha, S., Obermyer, R. T., Zande, B. J., Chandhok, V. K., Simizu, S. and Sankar, S. G. and Horton, J. A. (2002). Magnetic properties of the low-temperature phase of MnBi. **J. Appl. Phys.** 91: 8525.

Songsiriritthigul, C., Phana,k M., Mothong, N., Attarataya, J., Pramanpol, N., Supruangnet, R., Kuaprasert, B., Klysubun, W. and Poo-arporn, Y. (2016). BL7.2W: Macromolecular Crystallography (MX) at Synchrotron Light Research Institute. **The 10th Asia Oceania Forum for Synchrotron Radiation Research** (Shanghai: Shanghai Synchrotron Radiation Facility).

Studenikin, S. A., Golego, N. and Cocivera, M. (1998). Fabrication of green and orange photoluminescent, undoped ZnO films using spray pyrolysis. **J. Appl. Phys.** 84: 2287.

Suchea, M., Christoulakis, S., Katsarakis, N. and Kitsopoulos, T. (2007). Comparative study of zinc oxide and aluminum doped zinc oxide transparent thin films grown by direct current magnetron sputtering. **Thin Solid Films** 515: 6562.

Sudmuang, P., Krainara, S., Kongtawong, S., Tong-on, A., Suradet, N., Klinkhieo, S. and Klysubun, P. (2014). COMMISSIONING OF THE 2.4 T MULTIPOLE WIGGLER AND THE 6.5 T SUPERCONDUCTING WAVELENGTH SHIFTER AT SIAM PHOTON SOURCE **Proceedings, 5th International Particle Accelerator Conference** 7: 1192.

Marresearch Gmp (2001) The desktop beamline. Retrieved from http:// www.img.bio.uni-goettingen.de/ms-www/internal/manuals/mar345/dtb/introduction.htm#1.

Wang, H., Xu, J. W., Ren, M. F. and Yang, L. (2011). Transparent conductive Al-doped ZnO thin films grown at room temperature. **J. Vac. Sci. Technol. A** 29: 031505.

Widjonarko, N,. (2016) Introduction to advanced X-ray diffraction techniques for

polymeric thin films. **J. Coatings** 6: 54.

Wu, H. W., Yang, R. Y., Hsiung, C. M. and Chu, C. H. (2013). Characterization of aluminum-doped zinc oxide thin films by RF magnetron sputtering at different substrate temperature and sputtering power. **J Mater Sci: Mater Electron** 24: 166-177.

Xinyi, L., Yunlan, W., Weifeng, L., Guoshun J. and Changfei Z. (2012). Study of oxygen vacancies influence on the lattice parameter in ZnO thin film. **Materials Letters** 85: 25.

Yi-hua, S, Hai-lin, W., Jian, C., Liang, F. and Lei, W. (2016). Structural and optoelectronic properties of AZO thin films prepared by RF magnetron sputtering at room temperature **Trans. Nonferrous Met. Soc. China** 26: 1655.

Yunlan, W., Xinyi, L., Guoshun, J., Weifeng, L. and Changfei, Z. (2013). Origin of (103) plane of ZnO films deposited by RF magnetron sputtering. **J Mater Sci: Mater Electron**. 24: 3764-3767.

Zhang D. H., Yang T. L., Ma J., Wang Q.P., Gao, R. W. and Ma H. L. (2010). Preparation and properties of AZO thin films on different substrates. **Appl. Surf. Sci**. 20: 44.

# APPENDICES

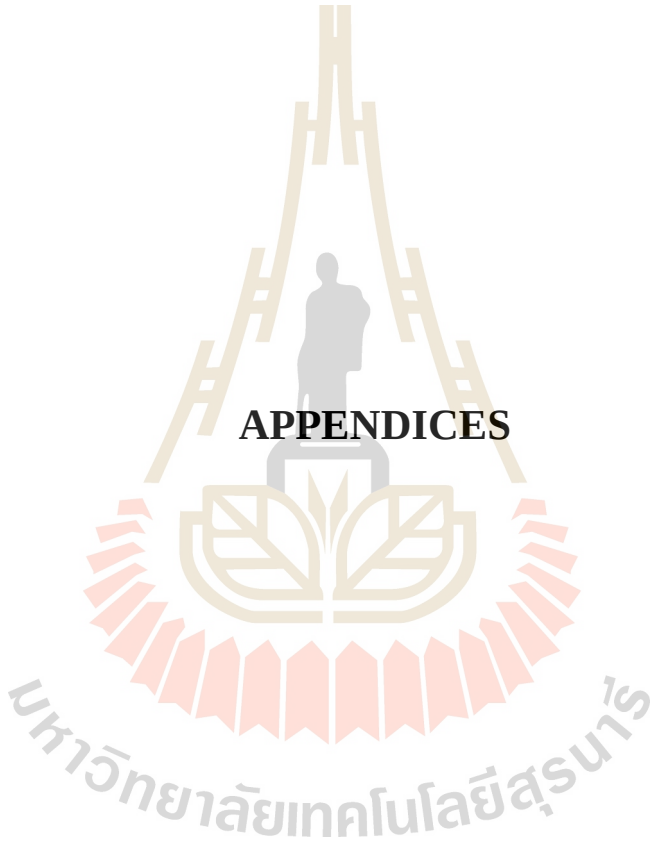

# APPENDIX A

# PATTERN ALIGNMENT AND CALIBRATION

In this work, the 2D GIXRD images were analyzed by using SAXSIT programs which was developed for small angle X-ray scattering data analyses (Rugmai, *et al.*, 2013). The procedures for GIXRD pattern alignment and standard calibration of a sample to detector distance (SDD) are given below.

a. Create a folder for raw to collect the data of measurement and the data that analyzed from SAXSIT programs. In this work, the 4-bromo benzoic acid was used as a calibration standard to determine the SDD and the position of primary beam.

b. Copy a location of the directory that was created before and paste into the "set working directory" (yellow box) in the main window of SAXSIT program as shows in figure A.1.

c. Click the "Analyze standard" button in the main menu window, the program will appear as a figure A.2.

d. In the "Load image" box, click the "browse" button and choose the 4-bromo benzoic acid data file to determine the position of the primary beam and calibrate SDD.

e. Click the "choose peak position" button in the "Approximate center" box and choose three point in 2$^{nd}$ diffracted ring of the interference of 4-bromo benzoic acid pattern. The first point should be started from the area which

is located closest to the beam stop shadow in the clockwise direction (figure A.3).

f. Specify the pixel size and type of the detector that was utilized, the X-ray energy, diffracted ring order and d-spacing of the standard (or click to select a type of standard) in the “Experimental parameters” box.

g. Click the “Run” in the “Search center and SDD Calibration” box. The program will determine the center position of the pattern by fitting all points in the diffracted from the first point to the end point in the clockwise direction (figure A.4).

h. Click the “Run” button again when the fitting is finished which will result in more accurate values.

i. Click the “Store results” button to store the data from 2$^{nd}$ diffracted pattern of the 4-bromo benzoic acid. Then repeat the fitting of the 2$^{nd}$ to 3$^{rd}$ and 4$^{th}$ diffracted rings from steps e-h again.

j. Click the “Average & Save” button in the “For multiple peaks” box. The program will provide the average fitting values from the three diffracted rings of the 4-bromo benzoic acid. The average fitting value i.e. i.e. Offset X, Offset Y, and SDD are saved in the “**alignstandard. txt**” file. The obtained are necessary for GIXRD data analysis**.**

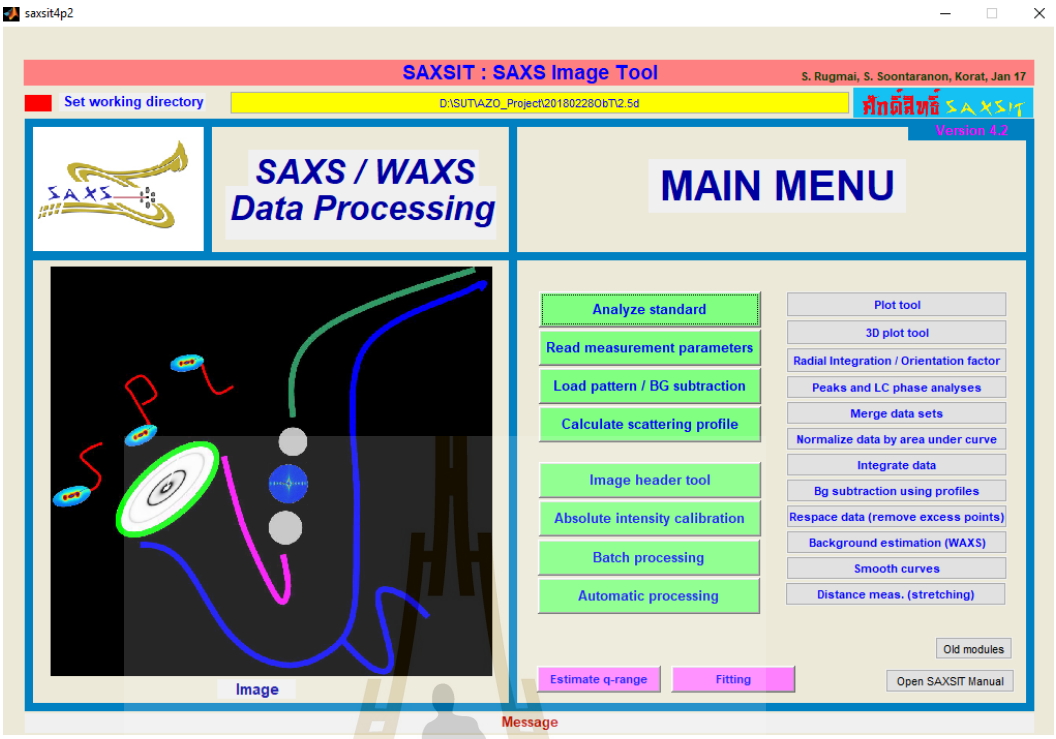


**Figure A.1** Main window of SAXSIT program.

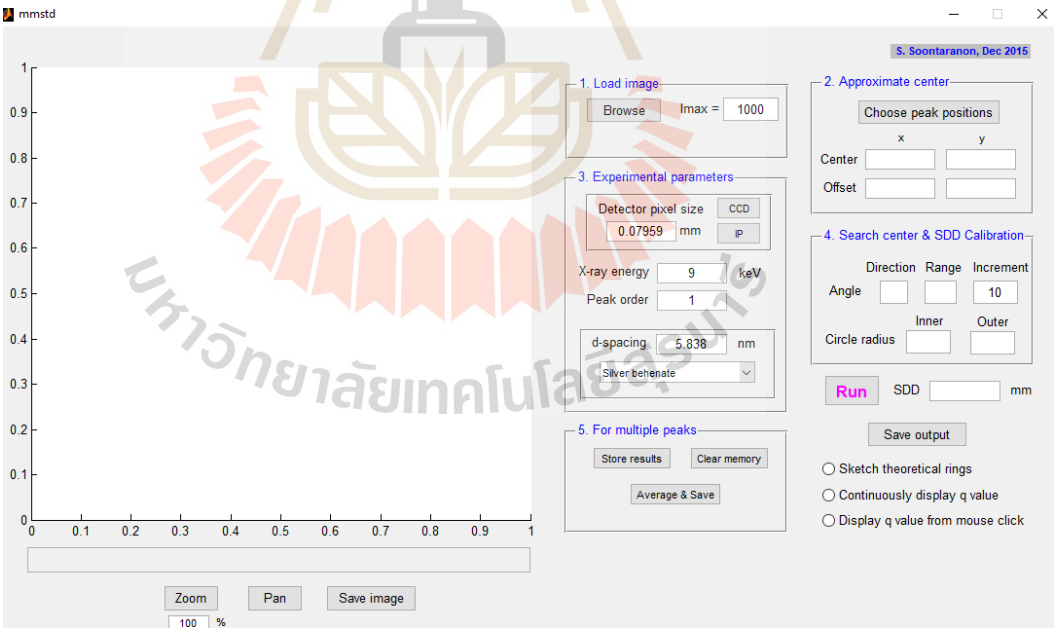


**Figure A.2** Analyze standard window of SAXSIT program.

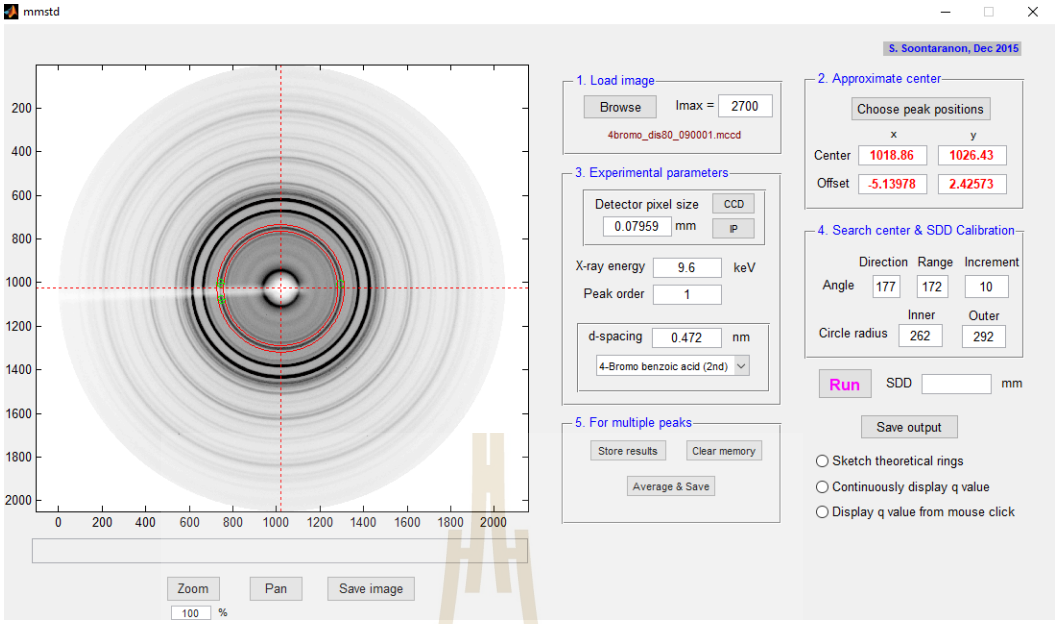


**Figure A.3** Analyze standard window with 2D diffraction image showing the selection of the position of the 2nd ring for estimating of the primary beam position.

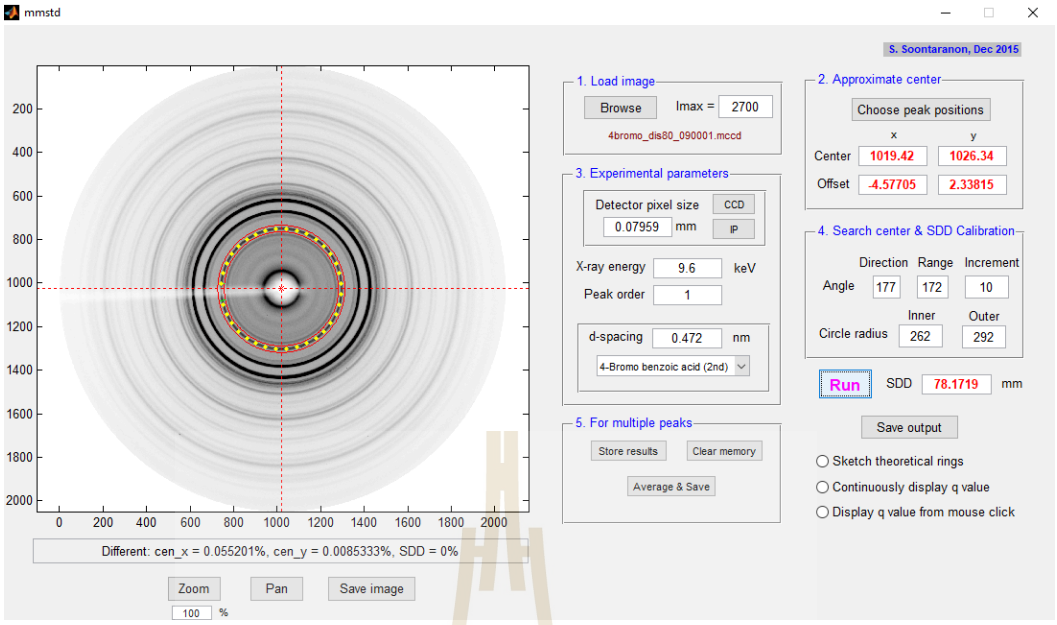


**Figure A.4** Analyze standard window with 2D diffraction image showing the selection of the position of the 2nd ring for estimating of the primary beam position after clicking the "Run" button.

# APPENDIX B

# GRAZING INCIDENCE X-RAY DIFFRACTION IN-SITU CELL

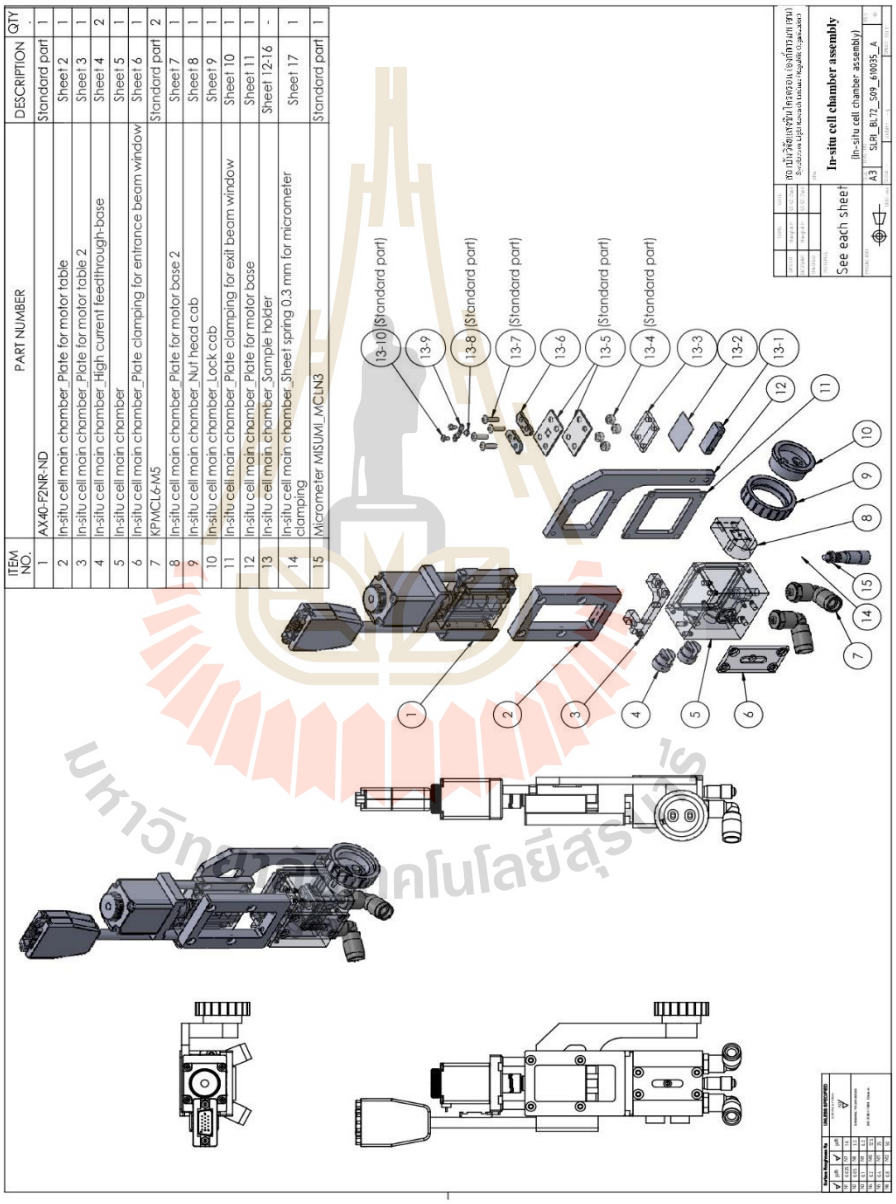


**Figure B** Exploded view drawing of the GIXRD in-situ cell.

# APPENDIX C

# PUBLICATION AND PRESENTATIONS

## C.1 List of Publication

Sripukdee, M., Songsiriritthigul, C., Mothong, N., Seawsakul, K., Saisopa1, T., Horprathum, T., and Songsiriritthigul P. (2018) Grazing Incident X-Ray Diffraction using Synchrotron Light at SLRI. **Journal of Physics Conf**. **Series** 1144

## C.2 List of Poster Presentations

Sripukdee, M., Songsiriritthigul, C., Mothong, N., Seawsakul, K., Saisopa1, T., Horprathum, T., and Songsiriritthigul P. (21018) Grazing Incident X-Ray Diffraction using Synchrotron Light at SLRI. In Siam Physics Congress 2018. Phitsanulok: Thai Physics Society.

Sripukdee, M., Seawsakul, K., Horprathum, M., Eiamchai, P., Limwichean, S., Songsiriritthigul, C., Mothong, N. and Songsiriritthigul, P. (2018) XRD investigations of AZO films prepared by DC pulsed magnetron sputtering. In 7 th International Symposium on Transparent on Conductive Materials (TCM 2018). Minoa Palace Hotel, Platanias, Chania, Crete, Greece.

Siam Physics Congress 2018 (SPC2018) : A Creative Path to Sustainable Innovation IOP Publishing
IOP Conf. Series: Journal of Physics: Conf. Series **1144** (2018) 012052 doi:10.1088/1742-6596/1144/1/012052

# Grazing Incidence X-Ray Diffraction using Synchrotron Light at SLRI

**M Sripukdee[1,2], C Songsiriritthigul[3], N Mothong[3], K Seawsakul[1], T Saisopa[1], M Horprathum[4], and P Songsiriritthigul[1,2]**

[1] School of Physics, Suranaree University of Technology, Nakhon Ratchasima 30000, Thailand,
[2] ThEP Center, Commission on Higher Education, Bangkok 10400, Thailand,
[3] Synchrotron Light Research Institute, Nakhon Ratchasima 30000, Thailand,
[4] Optical Thin-films Laboratory, National Electronics and Computer Technology Center, Pathumthani 12120, Thailand

E-mail : prayoon.song@gmail.com

**Abstract**. This work demonstrates the capability of the grazing incidence X-ray diffraction technique using synchrotron light. The measurement system is set up at the BL7.2W:MX beamline of the Synchrotron Light Research Institute (SLRI). The beamline utilizes hard X-rays from a 6.5-Tesla Superconducting Wavelength Shifter. The photon energy can be chosen between 7 to 18 keV with a photon flux of more than $10^{10}$ photons/sec at 100mA stored electron beam. The X-ray beam size can be reduced down to 20 microns, allowing XRD measurements in grazing geometry, thus crystal structures of very thin films with a thickness of tens nanometers can be identified. The diffraction patterns are recorded with a 2D CCD detector, allowing more diffraction spots of single crystalline films to be recorded.

## 1. Introduction

X-ray Diffraction (XRD) is one of well-known techniques for investigating structural properties of materials. When X-ray passed through a crystal, it would scatter off the atom in the sample and then produce constructive interference at specific angle. Conventional X-ray diffractometers (powder diffractometers) typically work on Bragg-Brentano geometry [1], the incident angle is defined between the X-ray source and the sample, the diffraction angle ($2\theta$) is defined between the incident beam and the reflect beam to the detector. In case of very thin films, grazing geometry is required to increase the interaction of X-ray with the materials in the films. The measurement with this geometry is known as grazing incidence XRD (GIXRD). GIXRD technique was first demonstrated by Marra et al. [2] for the study of crystalline surface and interface by varying the incidence angle of X-rays, which is typically very low angle, to get total X-ray external reflection from the sample. With GIXRD, the effective X-ray beam size on the sample surface is increased and the signal from a substrate is decreased [3]. X-ray from a synchrotron light source and from X-ray generator in laboratory may be employed for GIXRD measurements [4]. With the salient properties of synchrotron X-ray, there are several advantages when using synchrotron X-rays. The small size of synchrotron X-ray source allows GIXRD measurements to be performed in a small area on the sample. The intensity of synchrotron X-ray is much higher than rotating anode X-ray and, thus, the data collection time is much shorter when using synchrotron X-ray.

Siam Physics Congress 2018 (SPC2018) : A Creative Path to Sustainable Innovation IOP Publishing
IOP Conf. Series: Journal of Physics: Conf. Series **1144** (2018) 012052 doi:10.1088/1742-6596/1144/1/012052

It is well known that synchrotron X-ray has a continuous spectrum, thus, one can choose any X-ray wavelength suitable for the materials being investigated. In this work, a GIXRD technique was developed at the BL7. 2W:MX beamline of the Synchrotron Light Research Institute (SLRI). The measurement system was commissioned. The descriptions of the system and test results are given below.

## 2. Descriptions of BL 7.2W:MX Beamline

The beamline BL7.2W:MX utilizes synchrotron light produced from a 6. 5 Tesla superconducting wavelength shifter )SWLS( installed in the 1.2-GeV storage ring of the Siam Photon Source (SPS) of SLRI. The calculated synchrotron spectra generated from SWLS, as well as from other devices, i.e. a linear undulator with a period of 60mm (U60), Multi-Pole Wiggler (MPW) and Bending Magnet (BM), are shown in figure 1 [5]. The actual photon flux measured before entering the beam shaping slits of the XRD set up is shown in figure 2. It is clearly shown that the photon flux from 7 to 18keV range is in the order of $10^{10}$ photons/s, which is more than sufficient for general XRD measurements. The photon flux is varied with photon energy and maximum at about 8 keV. For GIXRD measurements, the beam size is reduced down to 20 microns by using the beam shaping slits in order to obtain small beam area on the sample

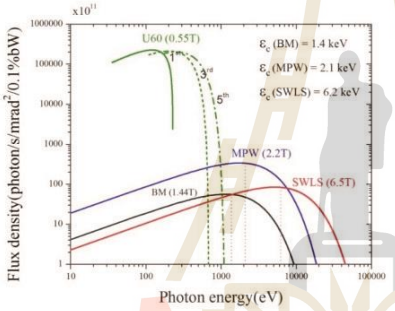


**Figure 1.** The SPS spectral flux densities [5]

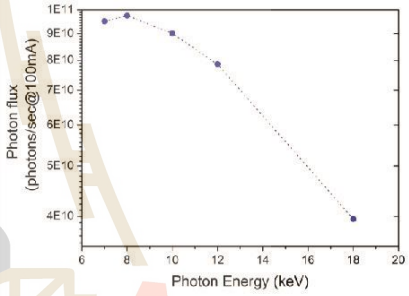


**Figure 2.** Measured photon flux before entering the beam shaping slits of the XRD measurement system.

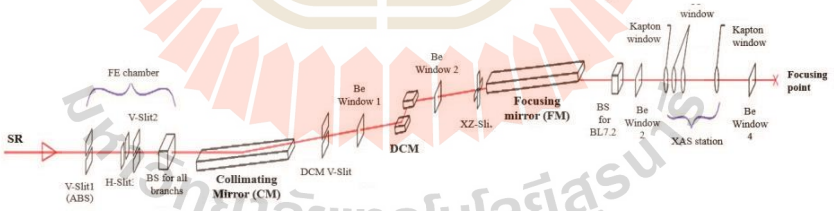


**Figure 3.** Optical layout of the BL7.2W: MX beamline

The optical layout of the BL7. 2W:MX beamline is shown in figure 3. Major optical elements of the BL7. 2W: MX beamline such as a cylindrical collimating mirror (CM), a commercial double-crystal monochromator (DCM) and a toroidal focusing mirror (FM) are used to obtain a focused hard X-ray beam with required characteristics for diffraction experiments of crystalline samples.

Siam Physics Congress 2018 (SPC2018) : A Creative Path to Sustainable Innovation IOP Publishing
IOP Conf. Series: Journal of Physics: Conf. Series **1144** (2018) 012052 doi:10.1088/1742-6596/1144/1/012052

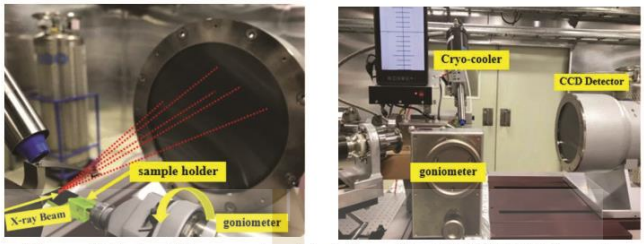


**Figure 4**. Photo of the experimental station of the BL7.2W:MX beamline.

Figure 4 shows the experimental station of BL7.2W: MX beamline which consists of cryo-cooler, sample holder and Mar165 CCD detector system (Rayonix LLC, Evanston, Illinois, USA). The sample holder and the detector are mounted on a MarDTB Goniometer system (Marresearch GmbH, Norderstedt, Germany). Taking the advantage of accurate controlling of a high precision phi-axis of MarDTB goniometer system, the sample can be tilted/rotated to adjust the angle of incidence between 0° to 360° with accuracy 0.002°. Thus, diffraction measurements with geometry is doable without any difficulties. The distance between the sample and detector can be varied between 45 to 390 mm. In addition, the detector can be rotated around the sample with the maximum angle of 30 degrees. The obtained 2D diffraction images may be processed with various 2D image processing computer programs, e.g. SAXSIT which was developed for small angle X-ray scattering data analyses [6].

## 3. Commissioning results and Discussion

The commissioning of the GIXRD set up was carried out on germanium antimony tellurium (GST) and aluminium doped zinc oxide (AZO) thin films prepared by using pulsed DC magnetron sputtering technique. The 4-bromo benzoic acid was used as a calibration standard to determine the accurate distance between the sample and detector. The diffraction images were collected using a monochromatic X-ray beam with a wavelength of 1.291 Å (9,600 eV) with an appropriate exposure time varying depending on the sample materials and sample-to-detector distance.

Figure 5(a) and (b) show the diffraction image taken from GTS and AZO thin films. Grazing incidence angle was fixed at 1.0° for GST thin film and 0.6° for AZO thin film, respectively. The distance of sample to the detector was fixed at 70 mm. The collection time for both samples was 2 min. The full Debye ring in figure 5(a) indicates that the X-ray beam falls on a sample of tiny crystals in all orientations, implying that the sample has a perfect polycrystalline texture [7]. Whereas the diffraction image taken from the AZO thin film appears as a partial ring, as in figure 5(b). Thus, this AZO film is not polycrystalline. The film was grown with a preferred orientation. With a 2D detector used at the beamline, one can collect diffracted beams in 2 dimensions. It is clearly shown in figure 5(c) by comparing data from the beamline and from a conventional system that some diffracted beams cannot be collected by a conventional laboratory GIXRD system using an X-ray tube.

The high intensity of synchrotron X-ray requires a short data collection time. The diffraction images/patterns in figure 5 were taken with collection time of 2 and 45 min at the synchrotron beamline and conventional GIXRD laboratory system, respectively. In addition to the advantage of a short data taking time, the synchrotron GIXRD can be carried with any X-ray wavelength from 7 to 18 keV, thus depending on specific requirements suitable for different sample materials.

Siam Physics Congress 2018 (SPC2018) : A Creative Path to Sustainable Innovation IOP Publishing
IOP Conf. Series: Journal of Physics: Conf. Series **1144** (2018) 012052 doi:10.1088/1742-6596/1144/1/012052

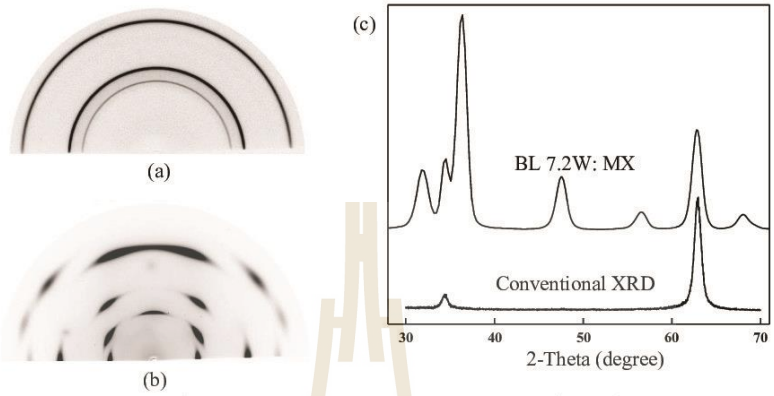


**Figure 5**. 2D GIXRD diffraction images of (a) GTS, (b) AZO thin films and (c) GIXRD patterns of AZO film measured at the BL7.2W:MX beamline (top) and conventional GIXRD system (bottom).

## 4. Conclusion

The advantages of synchrotron GIXRD at SLRI over conventional XRD systems have been demonstrated. Higher photon intensity and tunability of incident X-ray of synchrotron GIXRD are useful. In addition, a 2D detector available at the synchrotron beamline allows more types of materials to be investigated.

## References

[1] Kriegner D, Matěj Z, Kužel R and Holý V 2015 *J. Appl. Cryst.* **48** 613
[2] Marra W C, Eisenberger P and Cho A Y 1979 *J. Appl. Phys.* **50** 692
[3] Colombi P, Zanola P, Bontempi E, Roberti R, Gelfi M and Depero L E 2006 *J. Appl. Cryst.* **39** 176
[4] Neuschitzer M, Moser A, Neuhold A, Kraxner J, Stadlober B, Oehzelt M, Salzmann I, Resel R and Novak J 2012 *J. Appl. Cryst.* **45** 367
[5] Sudmuang P, Krainara S, Kongtawong S, Tong-on A, Suradet N, Klinkhieo S and Klysubun P 2014 *IPAC2014 Proc.* 7 1192
[6] Rugmai S and Soontaranon S 2013 *SAXSIT Manual* (Nakhon Ratchasima: Siam Photon Laboratory) ISBN 978-616-120274-3
[7] Widjonarko N 2016 *J. Coatings* **6** 54

Siam Physics Congress 2018

Abstract ID : 528

# Grazing Incident X-Ray Diffraction using Synchrotron Light at SLRI

## Content

This work demonstrates the capability of the BL7.2W:MX diffraction beamline at SLRI for investigation of crystallinity of nano-films. The beamline utilizes hard X-rays from a 6.5-Tesla Superconducting Wavelength Shifter, originally designed for protein crystallography. Its x-ray optical beamline employs a collimating mirror, double-crystal monochromator and focusing mirror. The photon energy can be chosen between 7 to 18 keV with a photon flux of more than 1010 photons/sec at 100mA stored electron beam. The X-ray beam size can be reduced to 20 micron, allowing X-ray diffraction (XRD) measurements with grazing geometry. The description of the synchrotron beamline and grazing incidence XRD (GIXRD) setup will be given with commissioning results. The advantages of synchrotron GIXRD will also be demonstrated in this work.

**Primary author(s) :** Ms SRIPAKDEE, Miskawan (Suranaree University of Technology)

**Co-author(s) :** Prof. SONGSIRIRITTHIGUL, Prayoon (Suranaree University of Technology)

**Presenter(s) :** Ms SRIPAKDEE, Miskawan (Suranaree University of Technology)

**Track Classification :** Instrumentation, Metrology and Standards

**Contribution Type :** Poster

Submitted by **SRIPAKDEE, Miskawan** on **Tuesday 10 April 2018**

TCM PS2-26

## XRD investigations of AZO films prepared by DC pulsed magnetron sputtering

Miskawan Sripakdee[1,2], Kittikhun Seawsakul[1], Mati Horprathum[3,a], Pitak Eiamchai[3], Saksorn Limwichean[3], Chomphunuch Songsiriritthigul[4], Narumol Mothong[4], Prayoon Songsiriritthigul[1,2,b]

[1]*School of Physics, Suranaree University of Technology, Nakhon Ratchasima, 30000, Thailand*
[2]*ThEP Center, Commission on Higher Education, Bangkok 10400, Thailand,*
[3]*National Electronics and Computer Technology Center, Pathum Thani, 12120, Thailand*
[4]*Synchrotron Light Research Institute, Nakhon Ratchasima, 30000, Thailand*
*Corresponding Author's E-mail: [a]mati.horprathum@nectec.or.th, [b]prayoon.song@gmail.com*

**Keywords:** aluminum-doped zinc oxide, pulsed dc magnetron sputtering, XRD, synchrotron x-ray.

**Abstract.** XRD technique using synchrotron X-ray with a 2-dimensional CCD detector was employed to investigate dense and columnar aluminum-doped zinc oxide (AZO) thin films on silicon (100) substrates. The thickness of the AZO films investigated is below 420 nm, and thus the measurements were carried out in a reflection mode with grazing angle varying from 0.5 to 10 degrees. The diffraction patterns collected by the CCD detector provide more information than those obtained from the conventional 1-dimensional XRD. The diffractions from the AZO films are not appeared as Debye rings, indicating that the films are not polycrystalline. The diffraction pattern was identified to be of a hexagonal wurtzite structure with c-axis preferably paralleled to the substrate normal. The XRD results show that some regions of the film materials were formed with the c-axis deviating from the substrate normal and, therefore, leading to angular broadening of the Bragg diffraction spots. The angular broadening increases with decreasing the grazing angle of the X-ray beam. In this work, the results from the analyses of the broadening and the diffraction intensity as a function of the grazing angle of the X-ray beam will be discussed and presented.

# CURRICULUM VITAE

**1. Name /Nationality:** Miss Miskawan Sripukdee / Thai

**2. Date & County of Birth:** 31 July 1991/ Thailand

**3. Education:** 2013, B.Sc. in Physics, Silpakorn University, Thailand

**4. Current Position**: Master student, School of Physics, Suranaree University of Technology, 111 University Avenue, Muang, Nakhorn Ratchasima 30000, Thailand

**5. Work experience:**

- **2014-2016** A teacher at Sarasas Wited Nakhorn Ratchasima school
- **2018** Master Student Research Assistant at BL 7.2W: MX beamline at Synchrotron Light Research Institute (Public Organization), Thailand.
- **2018-Present** Master Student Research Assistant at BL 1.1W: Multiple X-ray Techniques beamline at Synchrotron Light Research Institute (Public Organization), Thailand.

**6. Areas of Interest:**

- Investigations of materials using synchrotron radiation techniques.
- Development of X-ray diffraction using synchrotron radiation.